PALEOCEANOGRAPHY, VOL. 10, NO. 3, PAGES 373-394, JUNE 1995

A $\delta^{13}C$ record of Upper North Atlantic Deep Water during the past 2.6 million years

D. W. Oppo,[1] M. E. Raymo,[2] G. P. Lohmann,[1] A. C. Mix,[3] J. D. Wright,[4] and W. L. Prell[5]

Abstract. Benthic foraminiferal $\delta^{13}C$ data from site 502 in the Caribbean Sea (sill depth ~1800 m) indicate that throughout the past 2.6 m.y., glacial $\delta^{13}C$ values in the middepth Atlantic were higher during glaciations than interglaciations. This is interpreted as indicating a greater proportion of Upper North Atlantic Deep Water (UNADW) relative to southern source waters during glaciations. The contribution of UNADW during interglaciations to the middepth Atlantic remained approximately constant, and the contribution during glaciations may have been as much as 10 % higher in the late Pleistocene than in the late Pliocene. This small increase is in striking contrast to the much larger decrease in glacial Lower North Atlantic Deep Water (LNADW) contribution relative to southern sources, from about 80% to about 20%, that occurred over the past 2.6 m.y. Glacial intensification over the past 2.6 m.y. was probably coupled with a decrease in northward heat transport by the upper limb of the North Atlantic circulation cell, as was previously suggested on the basis of a LNADW record alone. Late Pleistocene (1 Ma-present) $\delta^{13}C$ values in the Caribbean Sea were approximately 0.2 ‰ higher than they were from 2.6 to 2.0 Ma. The $\delta^{13}C$ rise is not due to an increase in the mean ocean $\delta^{13}C$ value, nor can it be entirely attributed to an increase in the proportion of high-$\delta^{13}C$ source waters. An increase in the $\delta^{13}C$ value of the surface source waters must have contributed to the $\delta^{13}C$ rise.

Introduction

Over the past decade, a generalized model for late Quaternary glacial-interglacial changes in thermohaline circulation has emerged, largely based on carbon isotope ($\delta^{13}C$) and cadmium/calcium (Cd/Ca) values of benthic foraminifera from deep-sea cores. The utility of these two geochemical proxies is based on the observation that the distribution of $\delta^{13}C$ and Cd is correlated to that of nutrients in the modern ocean [e.g., *Kroopnick*, 1985; *Boyle*, 1988]. Low-$\delta^{13}C$ organic matter formed in surface water is oxidized and remineralized in the deep ocean, leaving high $\delta^{13}C$ values in nutrient-poor surface waters and lowering $\delta^{13}C$ values in deep, nutrient-rich waters. Like nutrients, Cd is depleted in surface waters, and its distribution is apparently also coupled to organic matter cycling (see review by *Boyle* [1988] and references therein). Thus, because the deep Atlantic Ocean is nutrient-poor relative to the Pacific Ocean, the deep Atlantic has higher $\delta^{13}C$ values and lower Cd concentrations than the deep Pacific.

Studies of $\delta^{13}C$ and Cd/Ca values of benthic foraminifera from upper Pleistocene sections of deep-sea cores have shown that during glaciations, the production of the deeper components (> 2 km) of North Atlantic Deep Water (Lower NADW; LNADW) is drastically reduced and that production of waters above 2 km, Upper NADW (UNADW), is enhanced [e.g., *Boyle and Keigwin*, 1987; *Curry et al.*, 1988; *Duplessy et al.*, 1988]. Modeling studies suggest that during glaciations, atmospheric circulation patterns resulting from the presence of the large North American ice sheets may have cooled North Atlantic surface waters [*Manabe and Broccoli*, 1985; *Keffer et al.*, 1988]. Thus, sea surface temperature (SST) variability may link ice volume and deep ocean circulation on glacial-interglacial timescales. With cooler surface waters and reduced evaporation, production of less dense UNADW may be favored over the production of LNADW [*Boyle and Keigwin*, 1987].

Studies of Plio-Pleistocene climatic and oceanographic evolution have built on the generalized model developed for the late Quaternary. Oxygen isotopic data and ice-rafted detritus (IRD) indicate that continental ice growth and regional cooling began in the northern hemisphere at ~3.2 Ma [*Berggren*, 1972; *Poore and Berggren*, 1975; *Shackleton and Opdyke*, 1977; *Keigwin*, 1987; *Keigwin and Thunnell*, 1979; *Loubere*, 1988; *Thunnell and Williams*, 1983; *Ruddiman et al.*, 1986; *Raymo et al.*, 1986, 1989], culminating at 2.57 m.y. BP with three glacial episodes having widespread IRD deposition in the open North Atlantic (stages 100, 98, and 96) and large increases in $\delta^{18}O$ [*Shackleton et al.*, 1984; *Raymo et al.*, 1989] (the chronology of

[1]Woods Hole Oceanographic Institution, Woods Hole, Massachusetts.
[2]Department of Earth, Atmospheric and Planetary Science, Massachusetts Institute of Technology, Cambridge.
[3]College of Oceanography, Oregon State University, Corvallis.
[4]Sawyer Environmental Research Center, University of Maine, Orono.
[5]Department of Geological Science, Brown University, Providence, Rhode Island.

Paper number 95PA00332.
0883-8305/95/95 PA-00332$10.00

Table 1. Locations of Cores Discussed in Text

Site	Latitude	Longitude	Depth, m	Region
849	0°N	111°W	3851	eastern equatorial Pacific
552	56°N	23°W	2301	middepth North Atlantic
607	41°N	33°W	3427	deep North Atlantic
502	11°N	80°W	3051	Caribbean Sea
610	54°N	18°W	2417	North Atlantic
643	68°N	1°E	2780	Norwegian Sea
644	67°N	4°E	1226	Norwegian Sea
677	1°N	84°W	3461	eastern equatorial Pacific

Data from the first four sites listed are the primary data sets for this study.

Shackleton et al. [1990] is used throughout this paper). The period between 1.2 and 0.7 Ma was a transition between relatively smaller glacial-interglacial ice volume variability of the Pliocene and early Pleistocene and the larger ice volume variability that characterized the late Pleistocene. The increase in the amplitude of the glacial-interglacial ice volume ($\delta^{18}O$) signal was associated with a change in the dominant periodicity of ice volume variability from 41 kyr (obliquity) prior to 0.7 Ma to 100 kyr after 0.7 Ma [*Prell*, 1984; *Ruddiman et al.*, 1989].

Down-core planktonic foraminiferal abundance changes and changes in interbasin carbon isotope gradients indicate that the evolution of the continental ice sheet system was accompanied by changes in North Atlantic SSTs and deepwater circulation. *Raymo et al.* [1990, 1992] examined changes in $\delta^{13}C$ gradients between the North Atlantic and deep Pacific over the past 3.2 m.y. using high resolution records from Deep Sea Drilling Project (DSDP) sites 552 (middepth North Atlantic) and 607 (deep North Atlantic) and Ocean Drilling Program (ODP) site 677 (deep equatorial Pacific) (Table 1, Figure 1). They documented an increase in the proportion of low-$\delta^{13}C$, nutrient-rich, Pacific-like waters in the deep North Atlantic which correlated with the gradual increase in glacial severity, although they also found that LNADW production was partially decoupled from ice volume on timescales longer than 100,000 years. In keeping with the late Quaternary model, *Raymo et al.* [1990] found that glacial suppression of LNADW was associated with reduced North Atlantic SSTs. These studies suggest that deepwater circulation may have played an important role in northern hemisphere cooling as reduced LNADW production must have been coupled with reduced northward heat transport in the upper limb of the North Atlantic thermohaline circulation cell throughout the last 3.2 Ma.

The history of UNADW over the past 1.2 m.y. was studied by *de Menocal et al.* [1992]. UNADW production was enhanced during glaciations relative to interglaciations as it was during the last glaciation [*Boyle and Keigwin*, 1987]. Generally, glaciations of greatest LNADW suppression as identified by *Raymo et al.* [1990] were associated with greatest relative UNADW contribution to the middepth North Atlantic, suggesting an out-of-phase behavior between UNADW and LNADW. In this study, we explore whether glacial-interglacial fluctuations in UNADW export to the middepth tropical Atlantic also occurred between 2.6 and 1.2 Ma and whether increasing glacial suppression of LNADW since 2.6 Ma [*Raymo et al.*, 1990] was

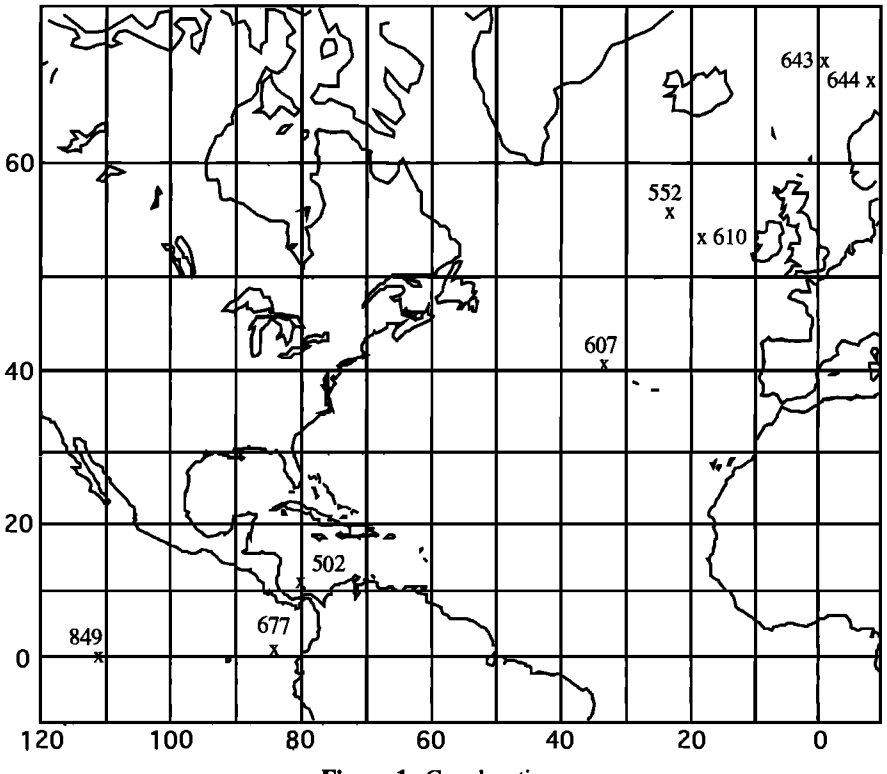

Figure 1. Core locations.

accompanied by increased production of UNADW, as might be predicted by the apparent tendency for the relative UNADW contribution to vary inversely with that of LNADW in the late Pleistocene. We also discuss long-term trends evident in the $\delta^{13}C$ records.

Data and Stratigraphy

To study changing oceanic $\delta^{13}C$ gradients through time, we use benthic foraminiferal carbon isotope records from several deep-sea sites (Table 1, Figure 1). We use the benthic foraminiferal isotope record from DSDP site 552 in the middepth North Atlantic to monitor changes in the $\delta^{13}C$ value of the nutrient-depleted, northern source water end-member. Whereas this core is located within the core of NADW today, during the last glaciation, site 552 was located in waters containing approximately 50% low-$\delta^{13}C$ southern source waters [*Oppo and Lehman*, 1993]. We use the record from ODP site 849 to monitor changes in the $\delta^{13}C$ value of Pacific Deep Water, the low-$\delta^{13}C$ end-member to the Atlantic via the Southern Ocean. Because the deep Pacific contains the greatest volume of the ocean's deep water, its $\delta^{13}C$ value is often assumed to be close to that of the mean ocean, and we make this assumption here. Variations in $\delta^{13}C$ at site 607, in the deep North Atlantic, are dominated by variations in the relative contribution of high-$\delta^{13}C$ NADW and low-$\delta^{13}C$ southern source waters to the deep Atlantic [*Raymo et al.*, 1990]. To these three records, we add a record from DSDP site 502 (Table 1), located on the Mono Ridge in the western Colombian Basin. Because the Caribbean Sea has an effective sill depth of 1800 m [*Wüst*, 1964], $\delta^{13}C$ values at this site should reflect $\delta^{13}C$ values in the middepth open Atlantic. Previous studies have shown that the Caribbean Sea contained more UNADW relative to southern sources during late Pleistocene glaciations than during interglaciations [*Boyle and Keigwin*, 1987; *Oppo and Fairbanks*, 1987, 1990; *de Menocal et al.*, 1992].

All four records are based primarily on the benthic foraminiferal species *Cibicidoides wuellerstorfi*, a species which in most regions appears to reliably record deepwater $\delta^{13}C$ values [e.g., *Belanger et al.*, 1981]. For the last 250,000 years of the site 607 composite record, *Ruddiman et al.* [1989] constructed a stack which included *Uvigerina* data from core V30-97 [*Mix and Fairbanks*, 1985] and *C. wuellerstorfi* data from core CHN82-4-24 [*Keigwin and Boyle*, 1985]. We have not removed the *Uvigerina* data since the main difference between the *Uvigerina* and *C. wuellerstorfi* data is that the *Uvigerina* $\delta^{13}C$ values were lower during the last glaciation; detailed comparisons of the late Pleistocene Caribbean Sea and deep North Atlantic records have been the subject of other studies [e.g., *Boyle and Keigwin*, 1987; *Oppo and Fairbanks*, 1987, 1990; *de Menocal et al.*, 1992] and are not the focus of this study. Some *Uvigerina* values are included in the site 849 record, and they also have not been removed since paired *C. wuellerstorfi* and *Uvigerina spp.* data indicate a constant down-core offset between the two species [*Mix et al.*, 1995]. Values of $\delta^{13}C$ of *Uvigerina spp.* are corrected to *C. wuellerstorfi* values and *C. wuellerstorfi* $\delta^{18}O$ values are corrected to *Uvigerina* values using correction factors given by *Shackleton and Hall* [1984]. The site 552 data have been published by *Shackleton and Hall* [1984] and *Curry and Miller* [1989]. The site 607 data are from *Ruddiman et al.* [1989] and *Raymo et al.* [1989, 1990, 1992]. The site 849 record is from *Mix et al.* [1995].

Most of the site 502 benthic isotope record above 1135 m (composite depth) was published by *de Menocal et al.* [1992]. A few additional measurements in this section have been made and are included in this paper (Table 2). The new data for site 502 were generated in two laboratories: at the Lamont-Doherty Earth Observatory (LDEO) on a Finnigan MAT251 with a common acid bath kept at 90°C and at the Woods Hole Oceanographic Institution (WHOI) on a Finnigan MAT252 with 70°C acid dropped into single reaction vessels. Samples from 44 depths were run in both laboratories. The difference between samples run in the two laboratories was 0.16 ± 0.18 ‰ (mean and 1σ) and 0.04 ± 0.15‰ for $\delta^{18}O$ and $\delta^{13}C$, respectively, with the WHOI laboratory giving the more positive values for both oxygen and carbon. Isotope data in both labs are calibrated through the use of standards from the National Bureau of Standards (NBS-20 at LDEO and NBS-19 at WHOI), so the reason for these differences is unclear. Because published values of the site 502 record were generated at LDEO, for continuity, we adjusted the WHOI values by subtracting 0.16 and 0.04 ‰ from $\delta^{18}O$ and $\delta^{13}C$ respectively.

The composite depth model for site 502 (Table 2), based on interhole correlations of sediments from holes 502, 502A, 502B, and 502C, is taken from W. L. Prell [manuscript in preparation, 1995]. Composite depths for the other cores are from the literature cited above and references therein [*Ruddiman et al.*, 1989; *Raymo et al.*, 1989, 1990, 1992; *Shackleton et al.*, 1990; *Mix et al.*, 1995]. The timescale for each core was generated by correlation of the benthic $\delta^{18}O$ record to the high-resolution record from Pacific ODP site 677, using the orbital chronology constructed by *Shackleton et al.* [1990]. Both the published [*de Menocal et al.*, 1992] and new $\delta^{18}O$ and $\delta^{13}C$ data of *C. wuellerstorfi* from site 502 are shown versus age in Figure 2 and listed in Table 2. The age model for site 502 is given in Table 3. Sedimentation rates vary little from the average rate of about 2 cm/kyr. With the exception of the interval between 2.1 and 1.7 Ma, when the site 502 $\delta^{18}O$ record exhibits very low amplitude fluctuations, correlation to other benthic isotope records was straightforward (Figure 3) and did not violate paleomagnetic constraints [*Kent and Spariosu*, 1982; *Shackleton et al.*, 1990].

The average sampling intervals (calculated after omitting data gaps of ~20 kyr or greater at sites 502 and 552) at sites 552, 502, 607, and 849 are approximately 6 kyr, 6 kyr, 4 kyr, and 4 kyr, respectively. Because of the large sampling interval at sites 552 and 502 and the large gaps that occur in these two records, we focus on long-term trends present in the data.

Results and Discussion

Oxygen Isotopes

The site 502 benthic oxygen isotope record provides no new insights beyond those already gleaned from the higher-resolution records (e.g., sites 607, 677, and 849 records [*Ruddiman et al.*, 1989; *Raymo et al.*, 1989, 1990, 1992; *Shackleton et al.*, 1990; *Mix et al.*, 1995]). The only significant difference between the sites 502 record and other oxygen isotope records that cannot be attributed to differences in resolution is the dampened amplitude of the $\delta^{18}O$ record from ~2.1 to 1.7 Ma, when the site 502 record appears to record only interglacial (low) $\delta^{18}O$ values. We know

Table 2. Isotope Data From Site 502

Core	Depth, cm	CDS, m	$\delta^{18}O$, ‰	$\delta^{13}C$, ‰	Lab
		C.wuellerstorfi			
1B-1	10.5	0.105	2.33	0.87	LDEO pub
1B-1	20.0	0.200	2.18	0.93	LDEO pub
1B-1	30.5	0.305	2.23	0.85	LDEO pub
1B-1	43.0	0.430	2.96	0.53	LDEO pub
1B-1	51.5	0.515	3.69	1.16	LDEO pub
1B-1	61.0	0.590	3.85	1.29	LDEO pub
1B-1	81.0	0.790	3.60	1.31	LDEO pub
1B-1	91.5	0.895	3.17	0.93	WHOI
1B-1	101.0	0.990	3.58	1.24	LDEO pub
1B-1	111.5	1.095	3.59	1.36	LDEO pub
1B-1	114.0	1.120	3.35	1.19	LDEO pub
1B-1	131.5	1.295	3.16	1.11	LDEO pub
1B-1	139.0	1.370	3.20	1.21	LDEO pub
1B-2	2.5	1.485	3.02	1.14	LDEO pub
1B-2	11.0	1.570	3.13	1.00	LDEO pub
1B-2	20.5	1.665	3.14	0.74	LDEO pub
2B-1	12.5	1.815	2.73	0.93	LDEO pub
2B-1	22.0	1.910	2.62	0.78	LDEO pub
2B-1	32.5	2.015	2.15	0.85	LDEO pub
2B-1	41.0	2.100	1.82	0.50	WHOI
2B-1	51.5	2.205	2.16	0.63	LDEO pub
2B-1	61.0	2.300	3.64	0.94	LDEO pub
2B-1	61.0	2.300	3.53	0.70	WHOI
2B-1	71.5	2.405	2.45	0.57	WHOI
2B-1	83.0	2.520	3.48	0.83	LDEO pub
2B-1	91.5	2.595	3.37	0.65	WHOI
2B-1	101.0	2.700	3.33	0.55	LDEO pub
2B-1	111.5	2.805	3.81	0.89	LDEO pub
2B-1	121.0	2.900	3.29	0.91	LDEO pub
2B-1	141.0	3.100	3.23	0.72	LDEO pub
2B-2	1.5	3.205	3.44	0.71	LDEO pub
2B-2	11.0	3.300	2.71	0.72	LDEO pub
2B-2	21.5	3.405	2.78	0.67	LDEO pub
2B-2	31.0	3.500	2.62	0.72	LDEO pub
2B-2	41.5	3.605	2.55	0.82	LDEO pub
2B-2	51.0	3.700	2.54	0.82	LDEO pub
2B-2	61.5	3.805	2.55	0.86	LDEO pub
2B-2	71.0	3.900	2.39	0.68	LDEO pub
2B-2	81.5	4.005	2.94	0.72	LDEO pub
2B-2	89.0	4.080	2.85	0.74	WHOI
2B-2	101.5	4.205	2.79	0.58	LDEO pub
2B-2	111.0	4.300	2.35	0.69	LDEO pub
2B-3	2.5	4.715	3.40	0.80	LDEO pub
2B-3	11.5	4.805	3.00	0.63	LDEO pub
2B-3	21.0	4.900	3.05	0.64	LDEO pub
2B-3	21.0	4.900	3.22	0.56	WHOI
2B-3	31.5	5.005	3.01	0.67	LDEO pub
2B-3	41.0	5.100	3.04	0.98	LDEO pub
2B-3	51.5	5.205	2.79	0.97	WHOI
3-1	10.5	5.210	3.19	1.06	LDEO pub
2B-3	61.0	5.300	2.76	0.82	LDEO pub
3-1	20.5	5.360	2.62	0.97	LDEO pub
2B-CC	6.5	5.405	3.37	0.84	LDEO pub

Table 2. (continued)

Core	Depth, cm	CDS, m	$\delta^{18}O$, ‰	$\delta^{13}C$, ‰	Lab
3-1	30.5	5.560	3.63	0.82	WHOI
3-1	49.5	5.750	2.65	0.80	LDEO pub
3-1	70.5	5.960	2.63	0.79	LDEO pub
3-1	90.5	6.160	2.55	0.76	LDEO pub
3B-1	11.5	6.215	2.57	0.75	WHOI
3B-1	11.5	6.240	2.44	0.68	LDEO pub
3B-1	21.0	6.310	2.31	0.75	LDEO pub
3-1	109.5	6.350	3.35	0.88	LDEO pub
3B-1	31.5	6.415	2.31	0.78	LDEO pub
3B-1	41.0	6.510	2.29	0.49	LDEO pub
3-1	130.5	6.560	2.54	0.75	LDEO pub
3B-1	51.5	6.615	2.47	-0.15	WHOI*
3B-1	61.0	6.710	3.59	0.69	LDEO pub
3-1	148.5	6.740	2.92	0.64	LDEO pub
3B-1	71.5	6.815	3.21	0.83	LDEO pub
3B-1	71.5	6.815	3.39	0.74	WHOI
3B-1	81.0	6.910	3.26	0.92	LDEO pub
3-2	19.5	6.950	3.14	0.71	WHOI
3B-1	91.5	7.015	3.39	1.08	LDEO pub
3B-1	101.0	7.110	3.14	0.93	LDEO pub
3-2	40.5	7.160	3.26	0.69	LDEO pub
3B-1	121.0	7.310	2.54	0.62	LDEO pub
3B-2	1.5	7.615	2.18	0.62	LDEO pub
3B-2	11.0	7.710	2.52	0.54	LDEO pub
3B-2	21.5	7.815	2.73	0.45	LDEO pub
3B-2	31.0	7.910	3.26	0.61	LDEO pub
3B-2	41.5	8.015	3.66	0.96	LDEO pub
3B-2	51.0	8.110	3.52	0.88	LDEO pub
3B-2	61.5	8.215	3.13	0.63	LDEO pub
3B-2	61.5	8.215	3.36	0.74	WHOI
3B-2	71.0	8.310	3.42	0.93	LDEO pub
3B-2	81.5	8.415	2.86	0.97	LDEO pub
3B-2	101.0	8.610	2.46	1.02	LDEO pub
3B-2	111.5	8.715	2.51	1.07	LDEO pub
3B-2	121.5	8.815	2.57	1.19	LDEO pub
3B-2	131.0	8.910	2.56	1.14	LDEO pub
3B-3	11.5	9.215	2.88	1.20	LDEO pub
3B-3	21.0	9.310	2.84	1.22	LDEO pub
3B-3	41.0	9.510	2.62	1.15	LDEO pub
3B-3	51.5	9.615	2.66	1.06	LDEO pub
3B-3	61.0	9.710	2.69	0.94	LDEO pub
3B-3	71.9	9.815	2.71	0.90	LDEO pub
3B-3	71.5	9.815	2.77	0.88	WHOI
3B-3	83.0	9.930	2.81	0.82	LDEO pub
3B-3	83.0	9.930	2.85	0.76	WHOI
3B-3	121.0	10.310	3.38	0.57	LDEO pub
4B-1	21.5	10.755	3.29	0.67	LDEO pub
4B-1	31.5	10.855	2.40	0.67	LDEO pub
4B-1	41.0	10.950	3.14	0.83	LDEO pub
4B-1	41.0	10.950	2.75	0.79	LDEO pub
4B-1	51.5	11.055	2.91	1.01	WHOI
4B-1	61.0	11.160	2.85	0.96	LDEO pub
4B-1	71.5	11.265	2.69	1.00	LDEO pub
4B-1	79.0	11.330	2.46	0.81	LDEO pub
4B-1	91.5	11.455	2.41	0.81	LDEO pub

Table 2. (continued)

Core	Depth, cm	CDS, m	$\delta^{18}O$, ‰	$\delta^{13}C$, ‰	Lab
4B-1	101.0	11.550	2.55	0.65	LDEO pub
4B-1	111.5	11.655	3.09	0.66	LDEO pub
4B-1	121.0	11.760	3.81	0.94	LDEO pub
4B-1	139.0	11.930	3.53	0.79	LDEO pub
4B-2	1.5	12.055	3.14	0.72	LDEO pub
4B-2	11.0	12.150	3.46	0.57	LDEO pub
4B-2	41.5	12.455	3.12	0.73	LDEO pub
4B-2	51.0	12.550	3.17	0.78	LDEO pub
4B-2	61.5	12.655	2.57	0.88	LDEO pub
4B-2	71.0	12.750	2.73	0.95	LDEO pub
4B-2	91.0	12.950	2.60	1.02	LDEO pub
4B-2	101.5	13.055	2.50	0.96	LDEO pub
4B-2	101.5	13.055	2.54	0.78	WHOI
4B-2	109.0	13.130	2.66	0.83	LDEO pub
4B-2	121.5	13.255	2.58	0.69	LDEO pub
4B-2	131.0	13.350	3.05	0.80	LDEO pub
4B-2	141.5	13.455	2.84	0.91	LDEO pub
4B-3	1.5	13.555	2.91	0.92	LDEO pub
4B-3	11.5	13.655	2.80	0.96	LDEO pub
4B-3	21.0	13.750	2.79	0.88	LDEO pub
4B-3	31.5	13.855	2.51	0.75	LDEO pub
4B-3	41.0	13.950	2.38	0.77	LDEO pub
4B-3	61.0	14.150	3.33	0.56	LDEO pub
4B-3	71.5	14.255	3.28	0.68	LDEO pub
4B-3	79.0	14.330	3.21	0.31	LDEO pub
4B-3	79.0	14.330	3.29	0.28	WHOI
4B-3	91.5	14.455	2.90	0.65	LDEO pub
4B-3	101.0	14.550	2.69	0.80	LDEO pub
4B-3	101.0	14.550	2.75	0.39	WHOI
4B-3	111.5	14.655	2.50	0.64	LDEO pub
4B-3	111.5	14.655	2.47	0.34	WHOI
4B-3	121.0	14.750	2.44	0.71	LDEO pub
4BCC	4.5	14.815	2.21	0.47	LDEO pub
5B-1	21.5	15.015	2.82	0.66	WHOI
5B-1	41.5	15.215	2.23	0.76	WHOI
5B-1	51.5	15.315	2.79	0.88	LDEO pub
5B-1	59.0	15.390	3.29	0.86	LDEO pub
5B-1	59.0	15.390	3.53	0.79	WHOI
5B-1	71.5	15.515	2.81	0.86	LDEO pub
5B-1	83.0	15.630	2.71	0.66	LDEO pub
5B-1	91.5	15.715	2.98	0.61	LDEO pub
5B-1	101.0	15.810	2.71	0.71	LDEO pub
5B-1	101.0	15.810	2.58	0.39	WHOI
5B-1	111.5	15.915	2.43	0.46	LDEO pub
5B-1	121.0	16.010	2.57	0.53	LDEO pub
5B-1	121.0	16.010	2.33	0.39	LDEO pub
5B-1	131.5	16.115	2.37	0.66	LDEO pub
5B-1	135.0	16.150	2.37	0.54	LDEO pub
5B-1	141.5	16.215	1.92	0.10	LDEO pub
5B-2	41.0	16.710	3.12	0.76	LDEO pub
5B-2	44.5	16.745	2.94	0.92	LDEO pub
5B-2	53.0	16.830	2.99	0.84	LDEO pub
5B-2	63.5	16.935	3.00	0.74	LDEO pub
5B-2	71.0	17.010	2.89	0.67	WHOI

Table 2. (continued)

Core	Depth, cm	CDS, m	$\delta^{18}O$, ‰	$\delta^{13}C$, ‰	Lab
5B-2	95.5	17.085	2.80	0.52	WHOI
5B-2	131.0	17.340	3.02	0.24	WHOI
5B-2	131.0	17.340	2.71	0.52	WHOI
5B-2	141.5	17.445	2.74	0.63	LDEO pub
5B-3	2.5	17.555	2.69	0.56	LDEO pub
5B-3	11.5	17.645	2.86	0.17	WHOI
5B-3	21.0	17.740	3.18	0.56	LDEO pub
5B-3	31.5	17.845	3.03	0.70	LDEO pub
5B-3	31.5	17.845	2.91	0.52	LDEO pub
5B-3	41.0	17.940	2.61	0.59	LDEO pub
5B-3	41.0	17.940	2.62	0.62	WHOI
5B-3	51.5	18.045	2.44	0.71	LDEO pub
5B-3	61.0	18.140	1.98	0.57	LDEO pub
5B-3	61.0	18.140	2.25	0.66	WHOI
5B-3	71.5	18.245	1.82	0.30	LDEO pub
5B-3	79.0	18.320	2.31	0.45	LDEO pub
5B-3	79.0	18.320	2.15	0.15	LDEO pub
5B-3	99.0	18.520	3.27	0.82	LDEO pub
5B-3	111.5	18.645	2.47	0.68	LDEO pub
5B-3	121.0	18.740	2.62	0.74	LDEO pub
5BCC	3.5	18.825	2.94	1.00	LDEO pub
6B-1	1.5	19.365	3.22	0.84	LDEO pub
6B-1	11.5	19.465	3.16	0.89	LDEO pub
6B-1	21.0	19.560	2.68	0.67	LDEO pub
6B-1	31.5	19.665	2.96	0.98	LDEO pub
6B-1	41.0	19.760	2.74	0.84	LDEO pub
6B-1	51.5	19.865	2.54	0.89	LDEO pub
6B-1	61.5	19.960	2.49	0.54	LDEO pub
6B-1	71.5	20.065	2.64	0.52	LDEO pub
6B-1	81.0	20.160	2.83	0.61	LDEO pub
6B-1	91.5	20.265	3.31	0.93	LDEO pub
6B-1	101.0	20.360	3.29	0.91	LDEO pub
6B-1	111.5	20.465	3.16	0.72	LDEO pub
6B-1	121.0	20.560	2.94	0.62	LDEO pub
6B-1	131.5	20.665	2.44	0.87	LDEO pub
6B-1	139.0	20.740	2.46	0.78	LDEO pub
6B-2	11.0	20.970	2.43	0.70	LDEO pub
6B-2	24.5	21.105	2.44	0.86	LDEO pub
6B-2	31.0	21.150	2.61	0.91	LDEO pub
6B-2	41.5	21.275	2.54	0.80	LDEO pub
6B-2	51.0	21.350	2.85	0.60	LDEO pub
6B-2	51.0	21.350	2.65	0.49	WHOI
6B-2	61.5	21.475	2.78	0.74	LDEO pub
6B-2	71.0	21.550	3.10	0.80	LDEO pub
6B-2	71.0	21.550	2.91	0.83	WHOI
6B-2	81.5	21.675	2.27	0.71	LDEO pub
6B-2	91.0	21.750	3.00	0.70	LDEO pub
6B-2	91.0	21.750	2.39	0.84	LDEO pub
6B-2	101.5	21.875	2.83	0.63	LDEO pub
6B-2	109.0	21.930	2.95	0.71	LDEO pub
6B-3	1.5	22.355	2.46	0.92	LDEO pub
6B-3	11.5	22.455	2.44	0.96	LDEO pub
6B-3	21.0	22.550	2.36	0.85	LDEO pub
6B-3	31.5	22.655	2.40	1.03	LDEO pub

Table 2. (continued)

Core	Depth, cm	CDS, m	$\delta^{18}O$, ‰	$\delta^{13}C$, ‰	Lab
6B-3	41.0	22.750	2.31	0.82	LDEO pub
6B-3	51.5	22.850	2.32	0.84	LDEO pub
6B-3	61.0	22.950	2.33	0.80	LDEO pub
6B-3	71.5	23.050	2.44	0.89	LDEO pub
6B-3	78.0	23.120	2.43	0.71	LDEO pub
6B-3	91.5	23.255	2.89	0.76	LDEO pub
6B-3	101.0	23.350	3.23	0.85	LDEO pub
6B-3	111.5	23.455	3.20	0.84	LDEO pub
6B-3	119.0	23.530	2.99	0.83	LDEO pub
6B-3	131.5	23.645	2.83	0.67	LDEO pub
7B-1	5.5	23.805	2.64	0.78	LDEO pub
7B-1	15.5	23.905	2.90	0.65	LDEO pub
7B-1	23.0	23.980	2.87	0.56	LDEO pub
7B-1	23.0	23.980	2.94	0.57	WHOI
7B-2	2.5	24.045	2.19	0.87	LDEO pub
7B-2	11.0	24.130	2.45	0.83	LDEO pub
7B-2	31.0	24.330	2.22	0.54	WHOI
7B-2	31.0	24.330	2.15	0.59	WHOI
7B-2	41.5	24.435	2.21	0.25	WHOI
7B-2	51.0	24.530	2.30	0.52	LDEO pub
7B-2	61.2	24.630	2.12	0.36	LDEO pub
7B-2	71.0	24.730	2.96	0.52	LDEO pub
7B-2	71.0	24.730	3.06	0.54	WHOI
7B-2	91.0	24.930	2.62	0.81	LDEO pub
7B-2	101.5	25.035	2.79	0.80	WHOI
7B-2	101.5	25.035	2.51	0.50	WHOI
7B-2	131.0	25.330	2.36	0.45	WHOI
7B-2	131.0	25.330	2.07	0.80	WHOI
7B-2	141.5	25.435	2.64	0.54	WHOI
7B-3	1.5	25.535	2.93	0.60	WHOI
7B-3	11.5	25.635	3.01	0.82	WHOI
7B-3	11.5	25.635	2.96	0.96	WHOI
7B-3	21.0	25.730	2.65	0.79	WHOI
7B-3	21.0	25.730	3.08	0.46	WHOI
7B-3	31.5	25.835	2.31	0.92	WHOI
7B-3	41.0	25.930	2.35	0.67	WHOI
7B-3	51.5	26.035	2.87	0.76	WHOI
7B-3	61.0	26.130	2.80	0.78	LDEO
7B-3	61.0	26.130	2.98	0.75	WHOI
7B-3	71.5	26.235	2.95	0.77	LDEO
7B-3	81.0	26.330	2.58	0.75	LDEO
7B-3	81.0	26.330	2.77	0.58	WHOI
7B-3	81.0	26.330	2.40	0.61	WHOI
7B-3	81.0	26.330	2.89	0.72	WHOI
7B-3	81.0	26.330	2.31	0.77	WHOI
7B-3	91.5	26.435	2.53	0.58	LDEO
7B-3	101.0	26.530	2.32	0.86	LDEO
7B-3	101.0	26.530	2.46	0.76	WHOI
7B-3	101.0	26.530	2.27	0.79	WHOI
7B-3	101.0	26.530	2.19	0.38	WHOI
7B-3	101.0	26.530	2.10	0.76	WHOI
7B-3	111.5	26.635	2.29	0.80	LDEO
7B-3	111.5	26.635	2.15	0.63	WHOI
7B-3	111.5	26.635	2.07	0.57	WHOI
7B-3	111.5	26.635	2.15	0.84	WHOI

Table 2. (continued)

Core	Depth, cm	CDS, m	$\delta^{18}O$, ‰	$\delta^{13}C$, ‰	Lab
7B-3	121.0	26.730	2.23	0.66	WHOI
7B-3	121.0	26.730	2.45	0.76	WHOI
7B-3	131.5	26.835	2.61	0.79	LDEO
7B-3	139.0	26.910	2.75	0.72	LDEO
7B-3	139.0	26.910	2.62	0.70	WHOI
7B-3	148.5	27.005	2.82	0.76	LDEO
7B-3	148.5	27.005	2.77	0.52	WHOI
7B-4	1.5	27.045	2.78	0.67	LDEO
7B-4	11.5	27.145	3.01	0.79	LDEO
7B-4	21.0	27.240	2.96	0.85	LDEO
7B-4	21.0	27.240	3.01	0.77	WHOI
7B-4	31.5	27.345	2.44	0.89	LDEO
7B-4	41.0	27.440	2.53	0.97	LDEO
7B-4	41.0	27.440	2.54	0.86	WHOI
7B-4	51.5	27.545	2.54	0.86	LDEO
7B-4	61.0	27.640	2.49	0.87	LDEO
7B-4	61.0	27.640	2.57	0.57	WHOI
7B-4	71.5	27.745	2.61	0.74	LDEO
7B-4	71.5	27.745	2.56	0.38	WHOI
7B-4	79.0	27.820	2.53	0.66	LDEO
7B-4	79.0	27.820	2.78	0.53	WHOI
7B-4	91.5	27.945	2.94	0.51	LDEO
7B-4	91.5	27.945	3.09	0.53	WHOI
7b-4	101.0	28.040	2.85	0.38	WHOI
7B-4	111.5	28.145	2.45	0.64	LDEO
7B-4	121.0	28.158	2.44	0.64	WHOI
8B-1	15.5	28.195	2.78	0.24	LDEO
8B-1	15.5	28.195	2.15	0.22	WHOI
8B-1	21.5	28.255	3.25	0.52	LDEO
7B-4	121.0	28.260	2.51	0.83	LDEO
8B-1	31.5	28.355	2.85	0.62	LDEO
8B-1	31.5	28.355	2.97	0.60	WHOI
7B-4	131.5	28.375	2.24	0.54	LDEO
8B-1	41.5	28.455	2.78	0.47	LDEO
8B-1	41.5	28.455	2.70	0.41	WHOI
8B-1	51.5	28.555	2.53	0.59	LDEO
8B-1	61.5	28.655	2.41	0.77	LDEO
8B-1	71.5	28.755	2.32	0.79	LDEO
8B-1	101.0	29.050	2.61	0.78	LDEO
8B-1	121.0	29.250	2.52	1.04	LDEO
8B-1	131.5	29.355	2.32	0.86	LDEO
8B-1	141.0	29.450	2.37	0.96	LDEO
8B-1	141.0	29.450	2.35	0.68	WHOI
8B-1	148.5	29.525	2.20	0.79	LDEO
8B-2	1.5	29.555	2.14	0.89	LDEO
8B-2	11.0	29.650	2.15	0.94	LDEO
8B-2	11.0	29.650	2.22	0.69	WHOI
8B-2	91.0	30.070	3.18	0.90	LDEO
8B-2	92.5	30.085	3.17	0.89	LDEO
8B-2	102.5	30.185	3.43	0.72	LDEO
8B-2	111.0	30.270	3.15	0.84	LDEO
8B-2	121.5	30.375	3.20	1.21	LDEO
8B-2	141.5	30.575	2.38	0.97	LDEO
8B-2	149.5	30.655	2.56	0.98	LDEO
8B-3	11.5	30.725	2.41	0.86	LDEO

Table 2. (continued)

Core	Depth, cm	CDS, m	$\delta^{18}O$, ‰	$\delta^{13}C$, ‰	Lab
8B-3	21.0	30.820	2.55	0.69	LDEO
8B-3	31.5	30.925	2.57	0.80	LDEO
8B-3	41.0	31.020	2.90	0.69	LDEO
8B-3	41.0	31.020	2.77	0.00	WHOI*
9-1	44.0	31.040	2.33	0.44	WHOI
8B-3	61.0	31.220	3.11	0.89	LDEO
9-1	84.0	31.440	2.49	0.74	WHOI
8B-3	101.0	31.620	2.71	0.80	WHOI
8B-3	101.0	31.620	2.18	0.77	WHOI
8B-3	101.0	31.620	2.47	0.75	WHOI
9-1	104.0	31.640	2.56	0.73	WHOI
8B-3	107.5	31.685	2.76	0.42	LDEO
8B-CC	3.5	31.705	2.71	0.65	LDEO
8B-CC	12.5	31.795	2.71	0.66	LDEO
9-1	124.0	31.840	2.25	0.78	WHOI
9-2	14.0	32.220	2.73	0.71	WHOI
9-2	14.0	32.220	2.93	0.41	WHOI
9-2	34.0	32.420	2.93	-0.05	WHOI*
9B-1	21.5	32.575	2.23	0.88	LDEO
9-2	54.0	32.620	2.54	0.73	WHOI
9B-1	31.5	32.675	2.56	0.86	LDEO
9B-1	51.5	32.875	2.63	0.43	LDEO
9B-1	61.0	32.970	2.53	0.97	LDEO
9B-1	61.0	32.970	2.45	0.59	WHOI
9B-1	71.5	33.075	2.41	0.79	LDEO
9-2	114.0	33.220	2.27	0.73	WHOI
9B-1	101.0	33.370	2.42	0.81	LDEO
9B-1	111.5	33.475	2.76	0.91	LDEO
9B-1	121.0	33.570	2.50	0.81	LDEO
9B-1	149.5	33.855	2.35	0.89	LDEO
9B-2	11.0	33.970	2.46	0.92	LDEO
9-3	44.0	34.020	2.22	0.76	WHOI
9B-2	21.5	34.075	2.49	0.87	LDEO
9B-2	31.0	34.170	2.94	0.94	LDEO
9-3	64.0	34.170	2.47	0.69	WHOI
9B-2	41.5	34.275	2.93	0.81	LDEO
9B-2	51.0	34.370	3.15	0.93	LDEO
9-3	84.0	34.370	3.21	0.93	WHOI
9-3	84.0	34.370	2.93	0.73	WHOI
9B-2	61.5	34.475	3.18	0.91	LDEO
9B-2	71.0	34.570	3.05	0.86	WHOI
9B-2	71.0	34.570	2.98	0.69	WHOI
9B-2	81.5	34.675	2.79	0.42	LDEO
9B-2	81.5	34.675	2.67	0.68	WHOI
9B-2	91.0	34.770	2.77	0.90	LDEO
9B-2	101.5	34.875	2.46	0.89	LDEO
9B-2	111.0	34.970	2.42	0.89	LDEO
9B-2	121.5	35.005	2.33	0.80	LDEO
9B-2	131.0	35.100	2.34	0.69	LDEO
9B-2	140.5	35.195	2.39	0.66	LDEO
9B-2	149.5	35.285	2.49	0.68	LDEO
9B-3	5.5	35.345	2.48	0.62	LDEO
10-1	64.0	35.440	2.11	0.64	WHOI
9B-3	16.0	35.450	2.61	0.51	LDEO
9B-3	16.0	35.450	2.50	0.44	WHOI

Table 2. (continued)

Core	Depth, cm	CDS, m	$\delta^{18}O$, ‰	$\delta^{13}C$, ‰	Lab
9B-3	31.5	35.545	3.15	0.69	LDEO
10-1	84.0	35.640	2.71	0.31	WHOI
10-1	84.0	35.640	2.73	0.33	WHOI
9B-3	51.5	35.745	2.48	0.51	LDEO
9B-3	61.0	35.840	2.46	0.47	LDEO
9B-3	61.0	35.840	2.52	0.50	WHOI
9B-CC	5.5	35.945	2.48	0.60	LDEO
9B-CC	5.5	35.945	2.46	0.46	WHOI
10-1	124.0	36.040	2.02	0.36	WHOI
10-1	124.0	36.040	2.43	0.37	WHOI
1C-1	8.0	36.080	2.47	0.52	WHOI
10-1	144.0	36.240	2.45	0.31	WHOI
10-1	144.0	36.240	2.45	0.53	WHOI
1C-2	21.0	36.330	2.14	0.38	WHOI
10-2	14.0	36.440	2.39	0.19	WHOI
10-2	14.0	36.440	2.56	0.67	WHOI
1C-2	42.0	36.540	2.34	0.49	WHOI
10-2	34.0	36.640	2.19	0.18	WHOI
10-2	34.0	36.640	2.07	0.21	WHOI
1C-2	61.0	36.730	2.07	0.33	WHOI
10-2	55.0	36.850	2.29	0.57	WHOI
1C-1	83.0	36.950	2.46	0.77	WHOI
10-2	72.0	37.020	2.18	0.69	WHOI
10-2	72.0	37.020	2.56	0.48	WHOI
1C-2	103.0	37.150	2.17	0.77	WHOI
10-2	94.0	37.240	2.07	0.71	WHOI
1C-2	121.0	37.330	2.20	0.60	WHOI
10-2	116.0	37.460	2.27	0.61	WHOI
1C-2	142.0	37.540	2.08	0.70	WHOI
10-2	134.0	37.640	2.15	0.49	WHOI
10-2	134.0	37.640	2.47	0.65	WHOI
1C-3	31.0	37.760	2.22	0.68	WHOI
1C-3	71.0	38.160	2.17	-0.04	WHOI*
10-3	44.0	38.250	2.23	0.55	WHOI
10-3	44.0	38.250	2.02	0.34	WHOI
1C-3	91.0	38.360	2.83	0.79	WHOI
1C-3	91.0	38.360	2.16	0.52	WHOI
10-3	64.0	38.450	1.74	0.35	WHOI
1C-3	112.0	38.570	2.58	0.82	WHOI
1C-3	112.0	38.570	2.17	0.60	WHOI
10-3	84.0	38.650	2.10	0.28	WHOI
10-3	104.0	38.850	2.02	0.38	WHOI
10-3	104.0	38.850	3.17	0.37	WHOI
10-3	124.0	39.050	2.45	0.30	WHOI
1C-4	22.0	39.140	2.18	0.67	WHOI
1C-4	41.0	39.340	2.57	0.40	WHOI
1C-4	61.0	39.540	2.47	0.71	WHOI
1C-4	61.0	39.540	2.46	0.91	WHOI
1C-4	83.0	39.760	2.42	0.67	WHOI
1C-4	83.0	39.760	2.35	0.69	WHOI
1C-4	101.0	39.940	2.24	0.90	WHOI
12A-1	81.0	40.490	2.26	0.88	WHOI
2C-1	21.0	40.510	1.77	0.35	WHOI
2C-1	41.0	40.710	2.20	0.58	WHOI
12A-1	121.0	40.890	2.04	0.80	WHOI

Table 2. (continued)

Core	Depth, cm	CDS, m	$\delta^{18}O$, ‰	$\delta^{13}C$, ‰	Lab
12A-1	121.0	40.890	2.43	0.98	WHOI
11B-1	61.0	41.450	2.13	0.75	WHOI
2C-1	143.0	41.710	2.27	0.81	WHOI
2C-1	143.0	41.710	2.16	0.80	WHOI
2C-2	11.0	41.910	1.97	0.55	WHOI
2C-2	51.0	42.310	2.28	0.78	WHOI
2C-2	51.0	42.310	1.79	0.35	WHOI*
2C-2	51.0	42.310	2.22	0.73	WHOI
11B-2	11.0	42.450	2.08	0.57	WHOI
2C-2	71.0	42.510	2.12	0.97	WHOI
11B-2	31.0	42.650	2.10	0.64	WHOI
2C-2	91.0	42.710	2.07	0.81	WHOI
2C-2	111.0	42.910	2.25	0.49	WHOI
12A-3	41.0	43.090	2.58	0.69	WHOI
12A-3	41.0	43.090	2.31	0.78	WHOI
2C-2	131.0	43.110	2.28	0.73	WHOI
12A-3	81.0	43.490	2.09	0.65	WHOI
11B-2	131.0	43.650	2.56	0.97	WHOI
11B-2	131.0	43.650	2.27	0.68	WHOI
11B-2	131.0	43.650	2.19	0.85	WHOI
2C-3	41.0	43.710	2.08	0.80	WHOI
2C-3	41.0	43.710	2.02	0.86	WHOI
2C-3	61.0	43.910	2.46	0.62	WHOI
2C-3	61.0	43.910	2.46	0.75	WHOI
2C-3	61.0	43.910	2.31	0.93	WHOI
2C-3	61.0	43.910	2.40	0.86	WHOI
11B-3	21.0	44.070	2.27	0.74	WHOI
2C-3	81.0	44.110	2.57	0.92	WHOI
2C-3	81.0	44.110	2.47	0.47	WHOI
2C-3	81.0	44.110	2.58	0.79	WHOI
11B-3	41.0	44.260	2.46	0.55	WHOI
11B-3	41.0	44.260	2.37	0.50	WHOI
11B-3	41.0	44.260	2.31	0.49	WHOI
11B-3	41.0	44.260	2.91	0.44	WHOI
2C-3	101.0	44.310	2.06	0.76	WHOI
2C-3	101.0	44.310	2.29	0.94	WHOI
2C-3	101.0	44.310	2.11	0.72	WHOI
2C-3	101.0	44.310	2.16	0.67	WHOI
11B-3	61.0	44.460	2.82	0.78	WHOI
2C-3	121.0	44.510	2.18	0.86	WHOI
11B-3	79.0	44.640	2.84	-0.07	WHOI*
3C-1	21.0	45.010	2.40	0.69	WHOI
3C-1	21.0	45.010	2.56	0.66	WHOI
3C-1	61.0	45.410	2.42	0.57	WHOI
3C-1	81.0	45.610	2.23	0.55	WHOI
3C-1	81.0	45.610	2.25	0.59	WHOI
3C-1	101.0	45.810	2.41	0.53	WHOI
3C-1	121.0	46.010	1.94	0.74	WHOI
3C-2	11.0	46.390	2.31	0.41	WHOI
3C-2	31.0	46.590	3.13	0.28	WHOI
3C-2	51.0	46.790	2.91	0.88	WHOI
3C-2	51.0	46.790	3.06	0.80	WHOI
3C-2	71.0	46.990	2.64	0.62	WHOI
3C-2	71.0	46.990	2.47	0.75	WHOI
3C-2	91.0	47.190	2.58	0.78	WHOI

Table 2. (continued)

Core	Depth, cm	CDS, m	$\delta^{18}O$, ‰	$\delta^{13}C$, ‰	Lab
3C-2	131.0	47.590	2.13	0.60	WHOI
3C-2	131.0	47.590	2.01	0.59	WHOI
3C-2	91.0	47.910	2.23	0.65	WHOI
3C-3	41.0	48.190	2.54	0.62	WHOI
3C-3	41.0	48.190	2.44	0.43	WHOI
13B-1	41.0	50.560	2.17	0.53	WHOI
13B-1	61.0	50.760	2.08	0.54	WHOI
13B-1	83.0	50.980	2.02	0.53	WHOI
13B-1	101.0	51.160	2.06	0.48	WHOI
13B-1	121.0	51.360	2.37	0.46	WHOI
13B-1	131.0	51.360	2.35	0.49	WHOI
13B-2	11.0	51.760	2.19	0.61	WHOI
13B-2	31.0	51.960	1.95	0.41	WHOI
13B-2	50.0	52.150	1.86	0.36	WHOI
13B-2	73.0	52.380	2.79	0.70	WHOI
13B-2	91.0	52.560	2.81	0.61	WHOI
13B-2	91.0	52.560	2.62	0.32	WHOI
13B-2	91.0	52.560	2.55	0.67	WHOI
13B-2	111.0	52.760	2.44	0.83	WHOI
13B-2	131.0	52.960	1.98	0.74	WHOI
13B-3	22.0	53.370	2.21	0.78	WHOI
13B-3	41.0	53.570	2.21	0.60	WHOI
13B-3	61.0	53.770	2.03	0.60	WHOI
13B-3	83.0	53.990	2.05	0.38	WHOI
13B-3	101.0	54.170	2.05	0.43	WHOI
13B-3	121.0	54.370	2.25	0.32	WHOI
14B-1	22.0	54.670	3.00	0.68	WHOI
14B-1	22.0	54.670	2.83	0.51	WHOI
14B-1	22.0	54.670	2.79	0.61	WHOI
14B-1	41.0	54.860	2.65	0.64	WHOI
14B-1	61.0	55.060	2.40	0.68	WHOI
14B-1	101.0	55.460	1.96	0.74	WHOI
14B-1	141.0	55.860	1.99	0.17	WHOI
14B-1	141.0	55.860	2.38	0.42	WHOI
14B-1	141.0	55.860	2.16	0.29	WHOI
14B-2	11.0	56.060	2.44	-0.02	WHOI*
14B-2	31.0	56.260	2.46	0.64	WHOI
14B-2	49.0	56.440	1.98	0.52	WHOI
14B-2	73.0	56.660	2.33	0.39	WHOI
14B-2	91.0	56.840	2.40	0.32	WHOI
14B-2	111.0	57.040	2.75	0.40	WHOI
14B-2	111.0	57.040	2.85	0.51	WHOI
14B-2	111.0	57.040	2.93	0.54	WHOI
14B-2	131.0	57.240	2.44	0.58	WHOI
14B-3	21.0	57.640	1.98	0.50	WHOI
14B-3	41.0	57.840	1.87	0.35	WHOI
14B-3	61.0	58.040	2.13	0.50	WHOI
14B-3	83.0	58.260	2.23	0.68	WHOI
14B-3	83.0	58.260	2.30	0.64	WHOI
14B-3	94.0	58.350	2.24	0.64	WHOI
14B-3	94.0	58.350	2.31	0.55	WHOI
15B-1	22.0	59.170	2.17	0.37	WHOI
15B-1	41.0	59.360	2.59	0.41	WHOI
15B-1	61.0	59.560	2.65	0.62	WHOI
15B-1	101.0	59.960	2.05	0.69	WHOI
15B-1	141.0	60.360	2.21	0.63	WHOI

Table 2. (continued)

Core	Depth, cm	CDS, m	$\delta^{18}O$, ‰	$\delta^{13}C$, ‰	Lab
		Uvigerina spp.			
1C-4	61.0	39.540	2.92	-0.20	WHOI
1C-4	83.0	39.760	2.96	-0.56	WHOI
2C-1	61.0	40.910	3.53	-0.61	WHOI
11B-1	21.0	41.050	3.16	-0.11	WHOI
2C-1	79.0	41.090	3.35	-0.19	WHOI
11B-1	41.0	41.250	3.05	0.02	WHOI
2C-1	101.0	41.310	2.98	-0.12	WHOI
11B-3	61.0	44.460	3.61	-0.12	WHOI
11B-3	79.0	44.640	3.67	-0.03	WHOI
11B-3	99.5	44.840	2.96	-0.21	WHOI
11B-3	121.0	45.060	3.05	-0.23	WHOI

The composite depth section (CDS) is taken from W. B. Prel (manuscript in preparation, 1995). The final column indicates where the data were generated (LDEO, Lamont-Doherty Earth Observatory; WHOI, Woods Hole Oceanographic Institution) and if they were previously published by *de Menocal et al.* [1992]. A constant has been subtracted from data generated at WHOI as discussed in text.

*Data points that were judged spurious and not included in the time series displayed in the figures.

from planktonic (e.g., site 502 (W. L. Prell, unpublished data, 1995) and benthic isotope records from other sites (Figure 3) and from IRD records [*Jansen and Sjøholm*, 1991; *Raymo et al.*, 1986] that glacial excursions occurred, so low $\delta^{18}O$ values and reduced amplitude of the record are not due to the absence of ice volume fluctuations. The most likely explanation for the reduced amplitude is that *C. wuellerstorfi* lived primarily during the warmer, relatively ice-free periods of the 2.1 to 1.7 Ma interval. This explanation is consistent with $\delta^{18}O$ measurements of *Uvigerina spp.* showing more positive, glacial-like values (Table 2, Figure 4). Thus, although we include data from this interval in most of our figures and analyses, we caution that like $\delta^{18}O$, the $\delta^{13}C$ measurements probably did not capture the full range of values that existed during this interval.

Isotopic Covariance

Carbon isotope data from sites 849, 552, and 502 are shown in Figure 5. Including the site 607 data rendered the figure unreadable, because the site 502 and site 607 records continually cross each other. Readers are referred to *Raymo et al.* [1990] to see a comparison of site 607 data to site 552 data. Because of the low resolution of the site 502 record, we forsake time series analysis and instead group data over discrete intervals to determine whether glacial-interglacial time scale variations in the contribution of high-$\delta^{13}C$ UNADW to the Caribbean Sea occurred over the past 2.6 m.y. Results of time series analysis of the higher resolution records from sites 607 and 849 have already been presented, and show high coherency and an approximate 180° phase difference between benthic $\delta^{18}O$ and $\delta^{13}C$ at both sites [*Raymo et al.*, 1990; *Mix et al.*, in press]. Time series analysis of the 1.2-0 Ma section of sites 502 and 552 was presented by *de Menocal et al.* [1992]. At site 502, $\delta^{18}O$ and $\delta^{13}C$ were approximately in phase at the 41-kyr cycle, whereas at site 552, maximum $\delta^{13}C$ lagged minimum $\delta^{18}O$ by about one-quarter wavelength.

Core data are summarized by analyzing the covariance between the $\delta^{18}O$ and $\delta^{13}C$ values from each core. The results are shown graphically as covariance ellipses [*Sokal and Rohlf*, 1969] (Figures 6, 7, and 8). The principal axis of each ellipse is the one line that describes the maximum dimension of variance in the $\delta^{18}O$ and $\delta^{13}C$ data. The minor axis (not shown), perpendicular to and bisecting the major axis at the mean of the data, represents the residual variance not described by the major axis. The ellipse circumscribes the one standard deviation region about the mean of the data. The more elongated the ellipse, the more variance is described by the principal axis. It is important to note that the variance this axis represents could be due either to a strong covariance between $\delta^{18}O$ and $\delta^{13}C$ or to disproportianally large variance in either $\delta^{18}O$ or $\delta^{13}C$. To distinguish between these two possibilities, we calculated the coefficient of determination, r_{12}^2, which is a measure of the variance shared by $\delta^{18}O$ and $\delta^{13}C$ [*Sokal and Rohlf*, 1969]. This coefficient is analogous and proportional to the squared correlation coefficient, r^2, used in regression analysis with only one random variable. Even when the principal axis describes a significant percentage of the variance, the r_{12}^2 values may be small if most of the variance occurs in one variable (i.e., if the slope is close to zero). Together, these quantities will help us characterize and assess the nature of the relationship between $\delta^{18}O$ and $\delta^{13}C$ at the different sites. The slope of the principal axis, the 95% confidence limits for the slope, the percent of the variance described by the principal axis , and the r_{12}^2 values for each $\delta^{18}O$-$\delta^{13}C$ data set are given in Table 4.

We begin by discussing two examples: the $\delta^{18}O$ and $\delta^{13}C$ data from sites 502 and 552 for the 0-1 Ma interval (Figures 6a and 6b, respectively). The slope of the primary axis is positive for site 502 and negative for site 552. The covariance ellipse describing the site 502 data is more elongated than the ellipse describing the site 552 data. The r_{12}^2 values indicate that this is a result of the stronger covariance between $\delta^{18}O$ and $\delta^{13}C$ at site 502. In addition, the 95% confidence interval for the slope is much smaller for site 502 than for site 552 (Table 4), as would be expected by a glance at the raw data. In order to evaluate the evolving relationship between $\delta^{18}O$ and $\delta^{13}C$ at each core site, we show the covariance ellipses and their principal axes for three discrete time intervals (Figures 7a-7d). To maintain clarity, we do not plot the data points on the figures, but hope that the examples provided have convinced the readers that the data are summarized reasonably well by the covariance ellipses and the statistics provided in Table 4.

The covariance ellipses describing the $\delta^{18}O$ and $\delta^{13}C$ data from site 849 (Figure 7a) show that high $\delta^{13}C$ values are associated with interglaciations, and low values with glaciations. Glacial-interglacial $\delta^{13}C$ variability in the deep Pacific Ocean is believed to be dominated by changes in the mean ocean $\delta^{13}C$ value, which varies as low-$\delta^{13}C$ carbon is transferred between the ocean and the terrestrial organic carbon reservoir [*Shackleton*, 1977]. The r_{12}^2 values of 0.23 to 0.36, measuring the shared variance, indicate that both $\delta^{18}O$ and $\delta^{13}C$ have contributed to the

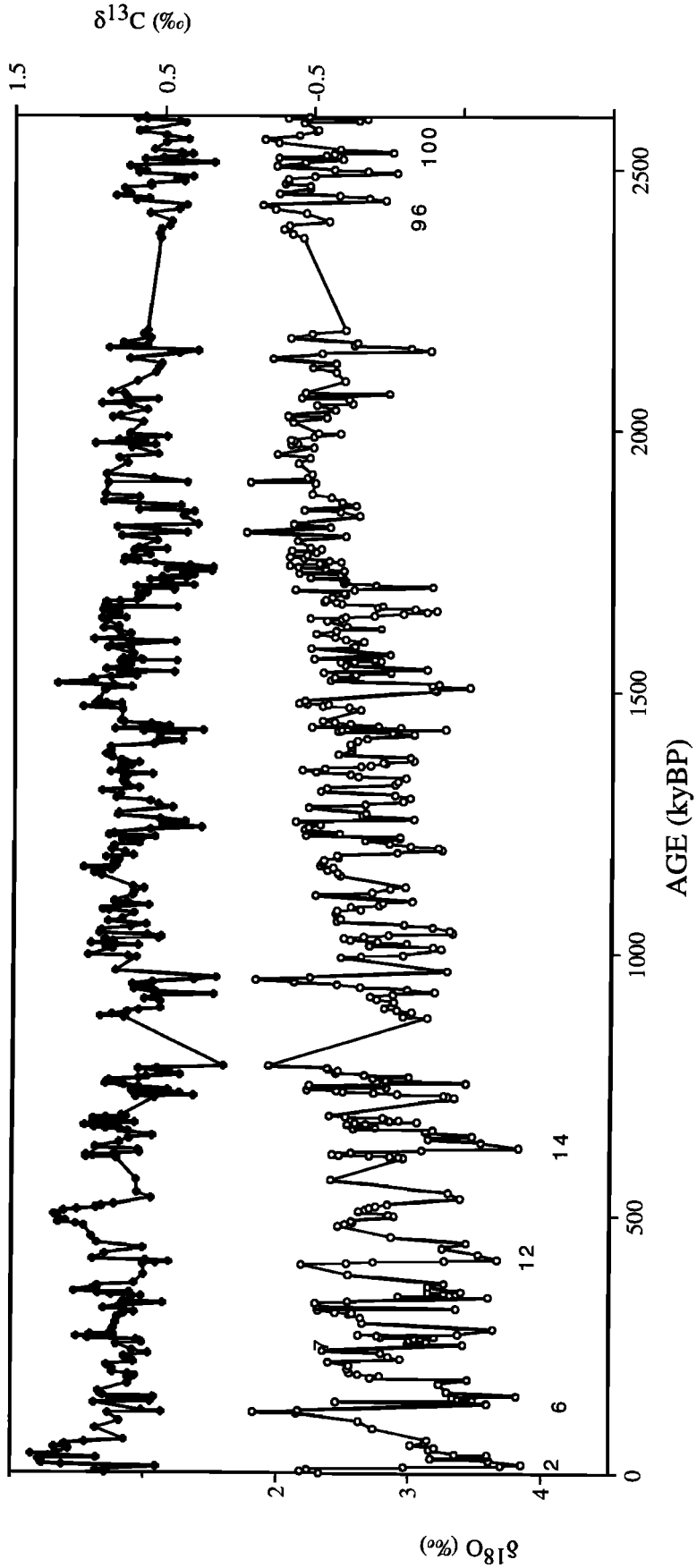

Figure 2. Values of $\delta^{18}O$ and $\delta^{13}C$ of the benthic foraminifera *Cibicidoides wuellerstorfi* versus age in site 502. Selected glacial stages are labeled.

Table 3. Age Model for Site 502

CDS, m	Age, ka
0.20	4
0.59	18
1.095	36
1.66	64
2.01	116
2.205	122
2.30	136
2.805	151
3.205	182
3.60	195
3.90	216
4.30	238
4.715	250
5.405	270
5.85	298
6.215	310
6.51	330
6.71	342
7.015	352
7.31	385
7.615	404.8
8.015	415
8.61	479
10.31	532
10.755	542.5
10.855	567
10.95	608
11.5	616
11.76	628
12.15	650
12.80	667
13.55	679
13.95	688
14.15	722
15.39	750
16.2	780
16.71	875
18.245	948
18.52	965.3
18.62	990
19.365	1008
20.265	1038
20.855	1071
21.55	1099
21.675	1110
21.93	1126
23.35	1196
24.435	1239
24.73	1255
25.33	1277
25.635	1295
25.93	1314
26.235	1334
27.145	1367
27.945	1417

Table 3. (continued)

CDS, m	Age, ka
28.755	1443
29.05	1464
29.555	1476
30.185	1507
31.22	1541
31.705	1558
32.42	1575
33.22	1610
33.855	1635
34.475	1655
35.1	1675
35.544	1701
36.95	1748
37.575	1770
38.25	1788
38.85	1836
41.85	1950
43.11	1992
44.46	2067
46.01	2134
46.59	2149
48.19	2188
50.56	2366
52.38	2438
54.67	2491
57.04	2530
57.84	2555
58.24	2571
59.56	2594
60.75	2600

high covariance (80%) throughout the past 2.6 m.y. The change through time of the slope of the major axes of the site 849 covariance ellipses is driven by the disproportionate increase in the amplitude of the $\delta^{18}O$ relative to the $\delta^{13}C$ signal; the amplitude of the $\delta^{13}C$ signal has not changed significantly despite increased ice volume variability and high covariance between $\delta^{18}O$ and $\delta^{13}C$.

Approximately 80% of the variation in $\delta^{18}O$ and $\delta^{13}C$ at site 502 is explained by the axis of their covariance during all three time intervals (Table 4). The low r_{12}^2 values (0.06 to 0.12) compared to the higher values at site 849 reflect the disproportionately low amplitude of the $\delta^{13}C$ record relative to that of the $\delta^{18}O$ record. Unlike the principal axes of the ellipses describing the data from sites 849, 607, and 552, (Figures 7a, 7c, and 7d), the principal axes of the site 502 data exhibit positive slopes (Figure 7b), showing a general tendency for higher $\delta^{13}C$ values to be associated with cooler periods (high $\delta^{18}O$) throughout the past 2.6 m.y. Thus from 2.6 to 1.2 Ma, glacial $\delta^{13}C$ values in the middepth tropical Atlantic were higher than interglacial values, just as they have been since [*Boyle and Keigwin*, 1987; *Oppo and Fairbanks*, 1987, 1990; *de Menocal et al.*, 1992].

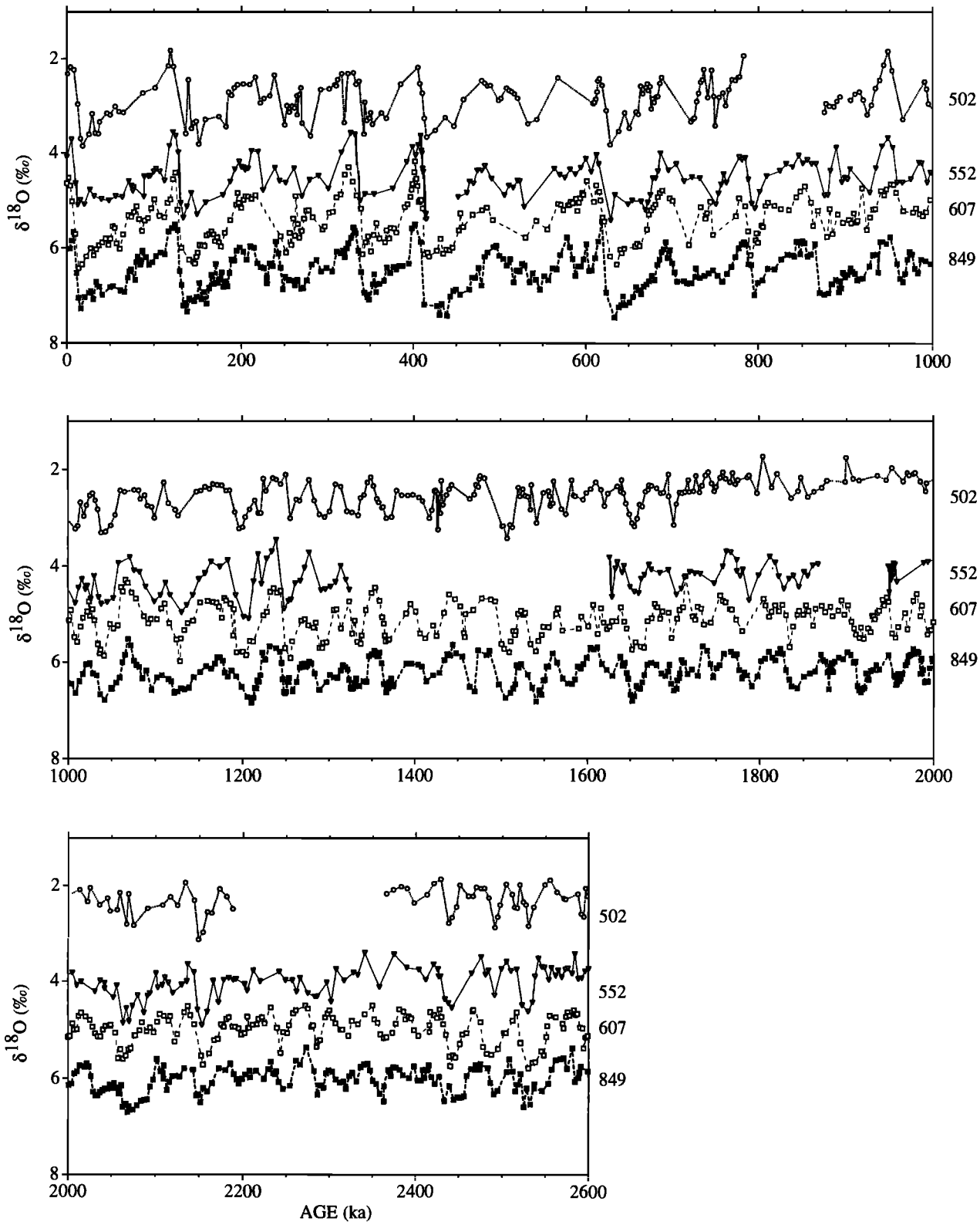

Figure 3. Records of $\delta^{18}O$ in benthic foraminifera from sites 849, 502, 552, and 607. Records are offset for clarity. Offsets from $\delta^{18}O$ values of *Cibicidoides wuellerstorfi* are 0‰, 1‰, 2‰, and 3‰ for sites 502, 552, 607, and 849, respectively. Except for the 2.1-1.7 Ma section, site 502 was easily correlated to the other records.

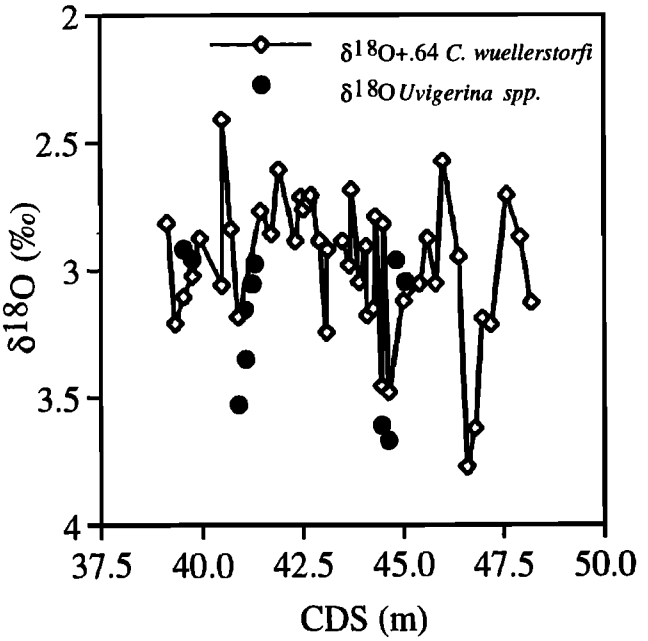

Figure 4. Values of $\delta^{18}O$ for the benthic foraminifera *Uvigerina species* and *Cibicidoides wuellerstorfi* for the depth interval corresponding to 2.1 to 1.7 Ma. A constant 0.64‰ has been added to the *Cibicidoides wuellerstorfi* values so that these values can be directly compared to *Uvigerina* values [*Shackleton and Hall*, 1984]. More negative *Cibicidoides wuellerstorfi* values after adjustment are consistent with the absence of glacial specimens.

The approximately constant slope of the principal axes through time at site 502 is rather striking. However, if the site 849 record is in fact close to the mean ocean $\delta^{13}C$ signal [*Mix et al.*, 1995], then the covariance ellipses that describe site 502 $\delta^{18}O$ versus site 502 minus site 849 $\delta^{13}C$ data ($\Delta\delta^{13}C(502\text{-}849)$) are a better description of the circulation imprint on the 502 $\delta^{13}C$ record. Because the site 849 data have negative covariance slopes, subtracting these data from the site 502 data steepens the positive slope of the principal covariance axis. The slopes of the major axes of the covariance ellipses adjusted for mean ocean $\delta^{13}C$ changes are similar for 1-2 Ma and 0-1 Ma but significantly different from the slope of the data from the 2-2.6 Ma interval (Figure 8a). The similarity of the slopes during the last two intervals suggests that at least over the past 2 m.y., increased glacial-interglacial ice volume variability was linearly coupled to an increase in $\delta^{13}C$ variability at site 502.

The negative slopes of the principal axes of covariance between the $\delta^{18}O$ and $\delta^{13}C$ data from site 849, 607 and 552 reflect the tendency for lower $\delta^{13}C$ values during glacial than interglacial stages at these deepwater sites (Figures 7a, 7c, and 7d). The principal axes describe between 75% and 85% of the covariance between the $\delta^{18}O$ and $\delta^{13}C$ data from sites 607 and 849, compared with only 65% of the data from site 552. For any given interval, the slope of the principal axis is less at site 552 than at the two other sites. The low covariance, shallow slope, large 95% confidence interval on the slopes, and low r_{12}^2 value at 552 for all three time intervals (Table 4) suggest that the tendency for lower glacial than interglacial $\delta^{13}C$ was weaker at 552 than at 607 and 849. In fact, the r_{12}^2 values approaching zero suggest that there is no consistent relationship between $\delta^{18}O$ and $\delta^{13}C$.

To explore this suggestion further, we examine the covariance between site 552 $\delta^{18}O$ and site 552 $\delta^{13}C$ with the mean ocean $\delta^{13}C$ signal removed (site 552 minus site 849 $\delta^{13}C$) (Figure 8b). The data indicate that relative to the mean ocean $\delta^{13}C$ value, site 552 has always had a tendency for higher glacial than interglacial $\delta^{13}C$ values. The slopes, covariances, and r_{12}^2 values suggest that this tendency has gradually weakened over the past 2.6 m.y. (Table 4).

It is likely that two factors contribute to the weak covariance between $\delta^{18}O$ and $\delta^{13}C$ at 552. The first of these is the absence of a 0°-phase or 180°-phase relationship between $\delta^{18}O$ and $\delta^{13}C$, which exists for the other sites [*Mix et al.*, 1995, *Raymo et al.*, 1990; *de Menocal et al.*, 1992]. The second, which we will discuss in more detail later in the paper, is the likelihood that site 552 was located close to the steep vertical gradient between nutrient-rich deep waters and nutrient-poor upper waters during past glaciations; subtle differences in surface forcing may result in vertical migration of the steep $\delta^{13}C$ gradient and the bathing of site 552 by waters having different $\delta^{13}C$ values. Which waters site 552 is bathed in depends on the relative location of site 552 with respect to the boundary between the high and low $\delta^{13}C$ water masses.

Thus covariance analysis indicates that of the four sites studied, site 502 is the only site to have consistently exhibited a general tendency for higher glacial than interglacial $\delta^{13}C$ values throughout the past 2.6 m.y. Subtracting the Pacific (site 849) record from the site 552 record, however, reveals that relative to the mean ocean $\delta^{13}C$ value, site 552 in the middepth North Atlantic has also experienced higher glacial $\delta^{13}C$ values. In the sections which follow, we discuss long-term $\delta^{13}C$ trends at sites 552 and 502 and the evolution of $\delta^{13}C$ gradients between the core sites. We also show that the higher glacial than interglacial $\delta^{13}C$ values at site 502 throughout the interval studied are probably due to a greater contribution of northern source waters during glaciations.

Long-Term $\delta^{13}C$ Trends

We took the mean and standard deviation of the $\delta^{13}C$ data from glacial and interglacial periods during the three time intervals to focus on long term trends in the average $\delta^{13}C$ values at each site and between sites (Figure 9, Table 5). An increase through time in $\delta^{13}C$ values is evident in the site 502 and 552 records (Figure 9). Site 607 $\delta^{13}C$ values are lower during the past 1 m.y. than they were earlier, due to the greater incursion of low-$\delta^{13}C$ southern source waters [*Raymo et al.*, 1990].

Possible reasons for the $\delta^{13}C$ increase at both sites 502 and 552 include (1) the mean ocean $\delta^{13}C$ value increased, (2) the sites experienced an increase in the contribution of high-$\delta^{13}C$ nutrient-depleted source waters, and (3) $\delta^{13}C$ values of source waters to the sites increased. A comparison of the site 502 and 552 records to the deep Pacific (site 849) record suggests that to the extent that the site 849 record represents changes in the mean ocean $\delta^{13}C$ value, the $\delta^{13}C$ increase at site 502 or site 552 may not be attributed to an increase in the mean ocean $\delta^{13}C$ value over the past 2.6 m.y. (Figure 9). If the predominantly *Uvigerina* $\delta^{13}C$ record from site 677 reflects the mean ocean $\delta^{13}C$ change better than does the predominantly *C. wuellerstorfi* record from site 849, then all of the $\delta^{13}C$ increase at sites 552 and 502 is

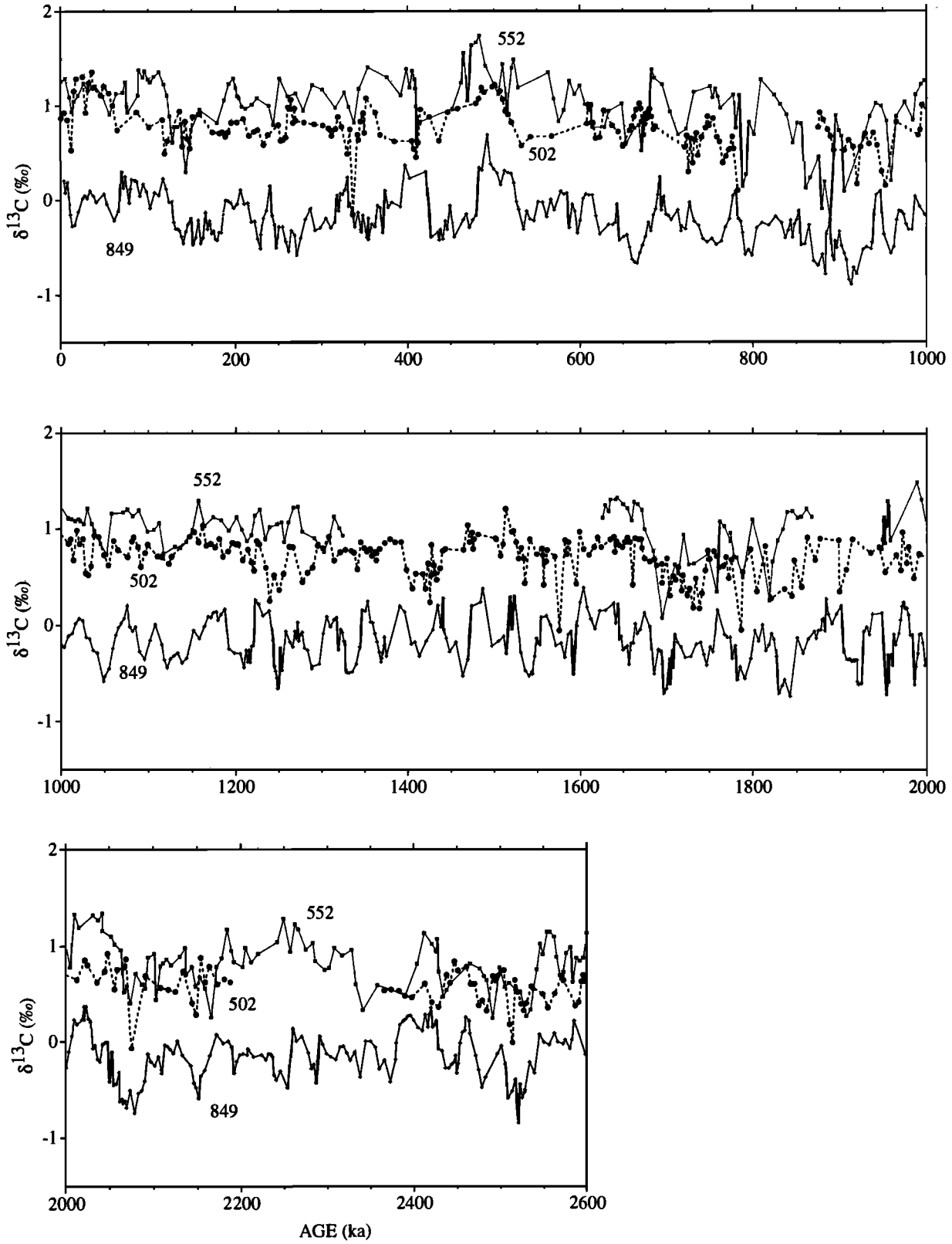

Figure 5. Records of $\delta^{13}C$ in benthic foraminifera from sites 849 (deep equatorial Pacific), 502 (Caribbean Sea), and 552 (middepth subpolar North Atlantic).

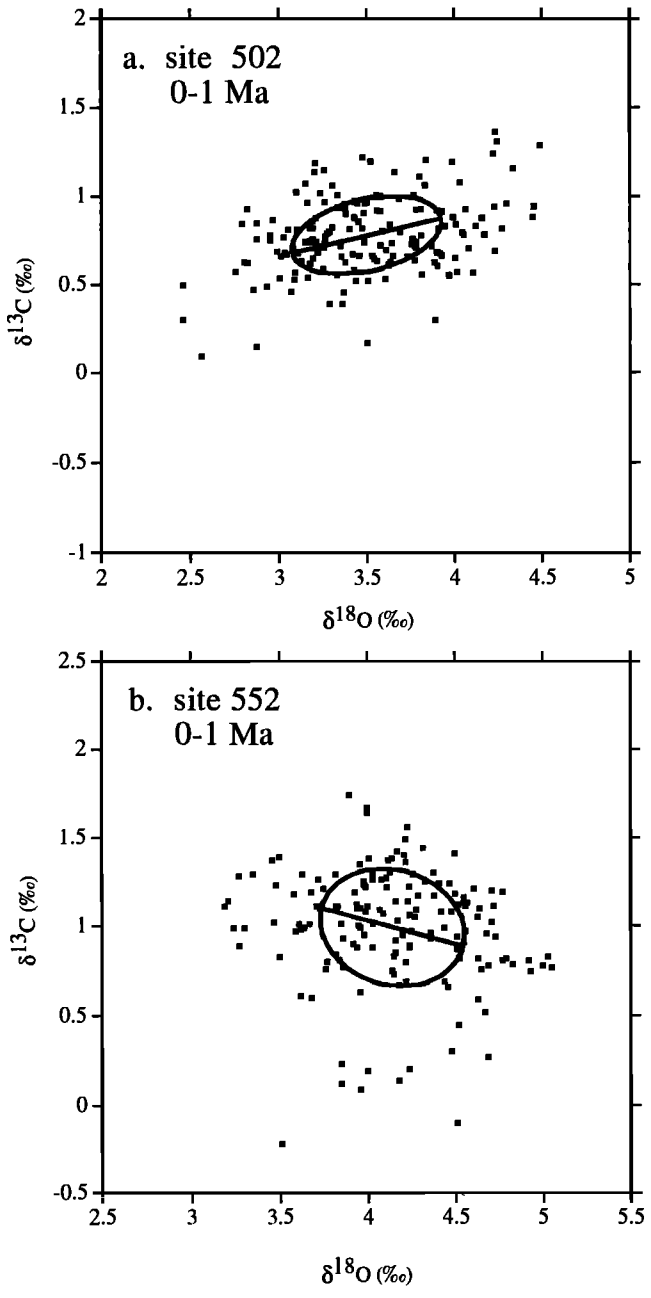

Figure 6. Covariance ellipses of the $\delta^{18}O$ and $\delta^{13}C$ data from sites (a) 502 and (b) 552 for the 0-1 Ma intervals. The data summarized by the variance ellipses are also shown. The principal axis of each ellipse describes the maximum variance between $\delta^{18}O$ and $\delta^{13}C$. The minor axis (not shown), perpendicular to and bisecting the major axis at the mean of the data, represents the residual covariance not described by the major axis. The ellipse circumscribes the one standard deviation region about the mean of the data. The more elongated the ellipse, the more variance is described by the principal axis [*Sokal and Rohlf*, 1969].

attributable to mean ocean $\delta^{13}C$ changes (Figure 9). The differences between the 677 and 849 $\delta^{13}C$ records are attributed to the open ocean location of site 849 compared to the location of 677 in the Panama Basin [*Mix et al.*, 1995]. *Mix et al.* [1995] suggest that bottom water $\delta^{13}C$ values in the Panama Basin are influenced by overlying high productivity and changes in the organic carbon flux to the sediments and that site 849 $\delta^{13}C$ values are therefore more representative of mean deep Pacific values. A low-resolution benthic isotope record from the western Pacific shows a small (0.1 ‰) decrease in $\delta^{13}C$ values over the past 2.6 m.y. [*Whitman and Berger*, 1990], but additional detailed Pacific $\delta^{13}C$ records are needed to confirm that the site 849 record is, as we believe, more representative of the mean ocean trend.

Was the $\delta^{13}C$ rise at sites 552 and 502 driven by an increase in the relative contribution of high-$\delta^{13}C$ northern source waters?

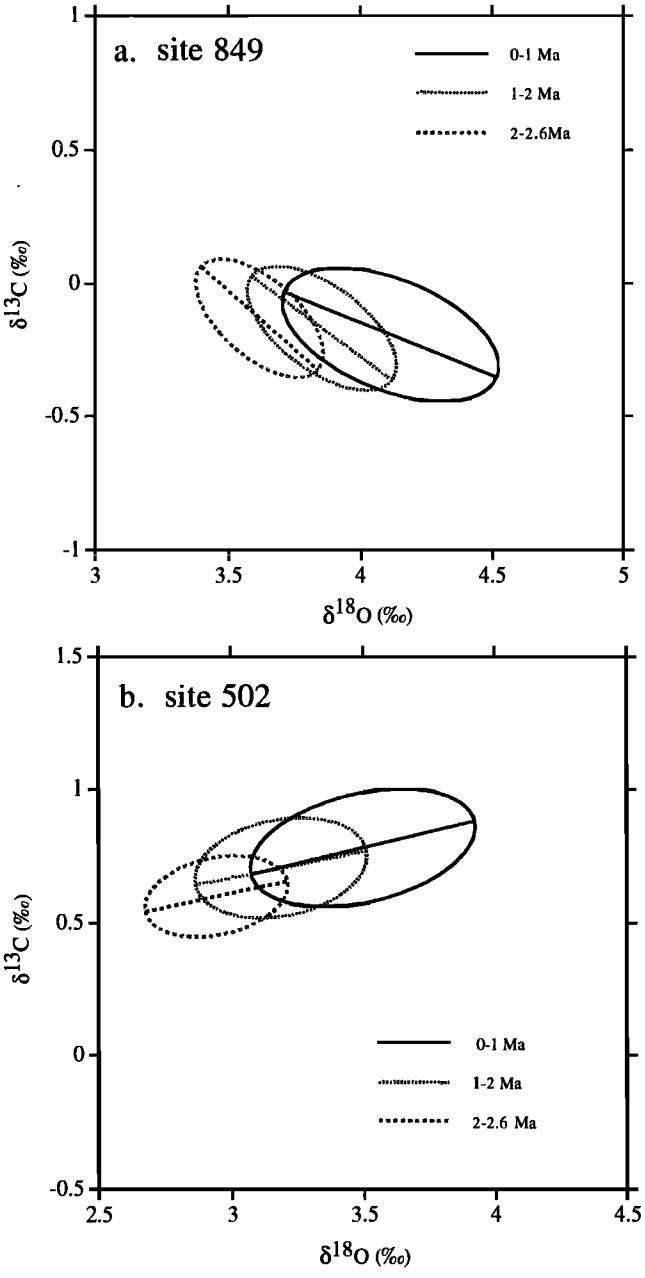

Figure 7. Covariance ellipses of the $\delta^{18}O$ and $\delta^{13}C$ data from sites (a) 849, (b) 502, (c) 607, and (d) 552. In each case, the major axis of the covariance axis is shown. Its slope and other relevant statistics are given in Table 4.

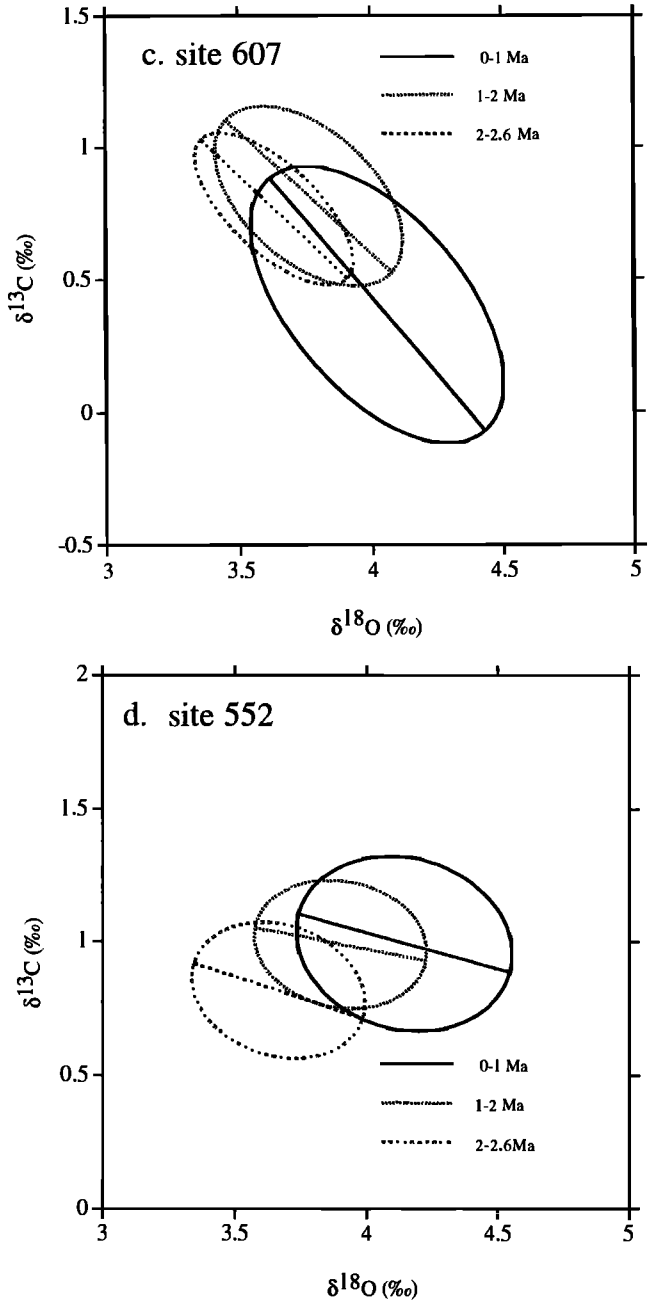

Figure 7. (continued)

Available data suggest that the northern source contribution to site 552 has been decreasing rather than increasing over the past 2.6 m.y. From 2.6 to 1.0 Ma, $\delta^{13}C$ values at site 552 were generally the same or higher than at sites 502 (Figure 5) and 607 [*Raymo et al.*, 1990], suggesting that it was located close to or within the core of NADW and thus the percentage of NADW to that site did not change significantly over that interval. However, over the last million years, $\delta^{13}C$ values were occasionally lower at site 552 than in the Caribbean Sea, for example near 875 ka, (Figure 5) and at other times in the past 150 kyr as identified with a higher-resolution Caribbean Sea record [*Oppo and Fairbanks*, 1990; *de Menocal et al.*, 1992]. At these times northern source waters probably formed either above or downstream of site 552, which was no longer within the core of nutrient-depleted source waters. During the last glaciation, the boundary separating high-$\delta^{13}C$ waters above from low-$\delta^{13}C$ waters below was located near a depth of 2000 m in the vicinity of site 552 on the Rockall Plateau [*Oppo and Lehman*, 1993]. At 2300-m water depth, site 552 was located in waters containing approximately 50% low-$\delta^{13}C$ southern source waters. Thus it appears that low-$\delta^{13}C$ southern source waters, not high-$\delta^{13}C$ nutrient-depleted source waters, have increasingly penetrated to this site during glaciations

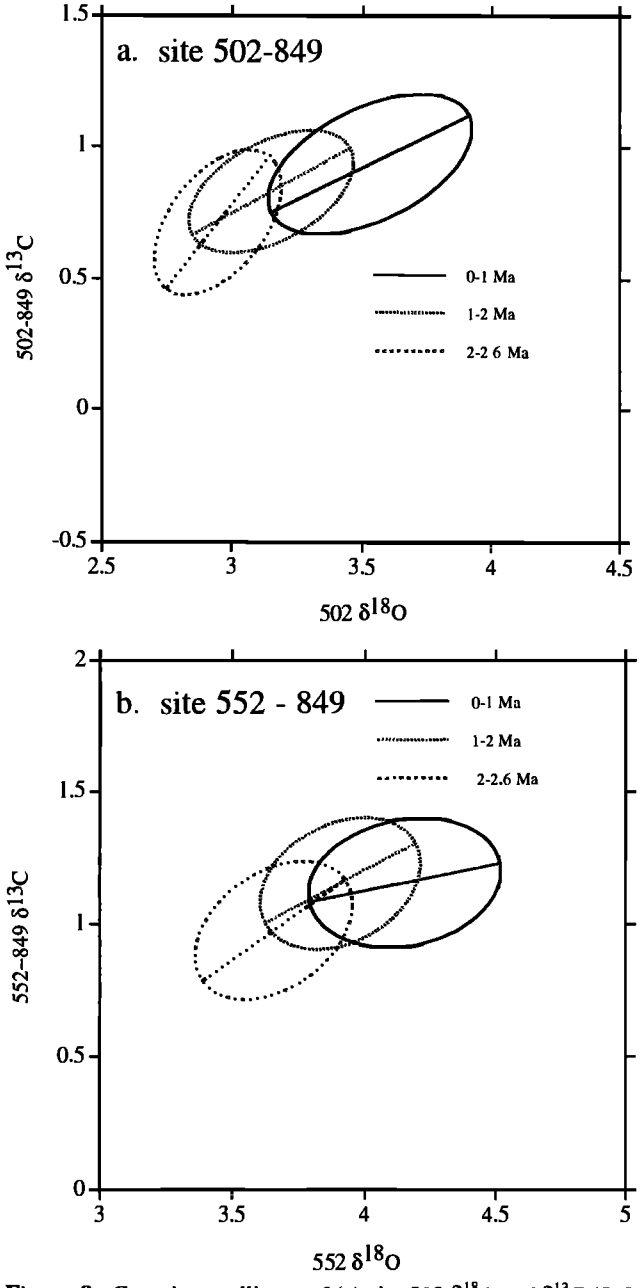

Figure 8. Covariance ellipses of (a) site 502 $\delta^{18}O$ and $\delta^{13}C$ (502 minus 849) and (b) site 552 $\delta^{18}O$ and $\delta^{13}C$ (552 minus 849). The major axis of the covariance axis is shown. Its slope and other relevant statistics are given in Table 4. The records were interpolated at 5,000-year intervals prior to subtraction, and sections with data gaps were omitted.

Table 4. Slopes of Major Axes of the Covariance Ellipses Describing $\delta^{18}O$ and $\delta^{13}C$ Data

Site	Region	Age, Ma								
		0 - 1			1 - 2			2 - 2.6		
		Slope	%Var	r_{12}^2	Slope	%Var	r_{12}^2	Slope	%Var	r_{12}^2
849	Pacific	-0.40 (-0.40, -0.39)	81%	0.23	-0.74 (-0.75, -0.73)	81%	0.36	-0.89 (-0.91, -0.87)	80%	0.36
607	deep North Atlantic	-1.17 (-1.20, -1.15)	78%	0.31	-0.93 (-0.95, -0.90)	75%	0.24	-0.96 (-0.98, -0.95)	84%	0.47
607- 849		-0.91 (-0.94, -0.88)	75%	0.24	-0.27 (-0.33, -0.21)	65%	0.03	-0.59 (-0.66, -0.52)	68%	0.11
502	Caribbean	0.23 (0.22, 0.24)	82%	0.12	0.20 (0.18, 0.21)	77%	0.06	0.22 (0.18, 0.25)	78%	0.07
502- 849		0.48 (0.47, 0.50)	80%	0.25	0.54 (0.54, 0.55)	78%	0.24	1.27 (1.19, 1.36)	76%	0.25
552	North Atlantic	-0.27 (-0.37, -0.18)	63%	0.02	-0.19 (-0.27, -0.11)	66%	0.01	-0.32 (-0.43, -0.22)	65%	0.03
552- 849		0.20 (0.17, 0.23)	71%	0.03	0.53 (0.46, 0.61)	67%	0.09	0.71 (0.64, 0.79)	70%	0.14

95% confidence interval for the slopes are given in parentheses. %Var is the percent variance accounted for by the principal axis, and r_{12}^2 is the coefficient of determination.

as climate deteriorated, and an increasing proportion of northern component water cannot account for the $\delta^{13}C$ rise at the site.

To evaluate whether the $\delta^{13}C$ increase through time at site 502 was due to increase in the contribution of northern source waters to the site, we should examine the evolution of the percentage of UNADW at 502 ($\%UNADW_{502}$) relative to southern source waters, calculated using $\delta^{13}C$ records from cores located in the core of the northern and southern end-member water masses [e.g., *Oppo and Fairbanks*, 1987; *Raymo et al.*, 1990].

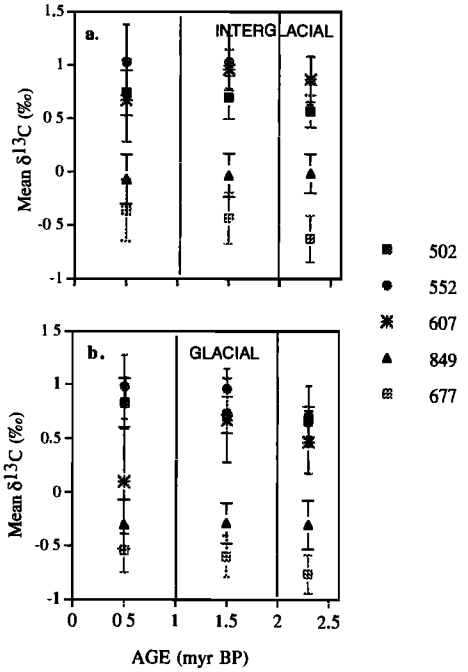

Figure 9. Mean $\delta^{13}C$ data from sites 849, 552, 607, 502, and 677 for (a) interglaciations and (b) glaciations for time intervals corresponding to the ellipses shown in Figure 7. The mean $\delta^{13}C$ data and one standard deviation are given in Table 5. Mean values for sites 607 and 502 are offset on the time axis for clarity.

Convincing results require high-resolution records with excellent correlation between them. At present, sites 552 and 849 are the best available northern and southern source end-member cores, respectively, although as we have discussed above, site 552 has probably been influenced by southern source waters over the past 1 m.y., making it a less than ideal end-member core. When the location of site 552 contains some southern source waters, we underestimate the proportion of UNADW at 502. In addition, a core from Upper Circumpolar Deep Water would have been a much better end-member than site 849, which is located in the Pacific Ocean. Although an isotope record from middepth South Atlantic site 704 is available, the site lies close to the core of NADW, and benthic foraminiferal $\delta^{13}C$ data from that site indicate that it too has been influenced by variable input of NADW and southern ocean water [*Hodell*, 1993; *Hodell and Venz*, 1992]. Finally, precise correlation between sites 849, 552, and 502 is difficult due to the low resolution of the site 552 and 502 records. Despite the shortcomings of the available data sets, dramatic changes, if they occurred, should be evident in a $\%UNADW_{502}$ record.

The $\%UNADW_{502}$, relative to deep Pacific water, is estimated by interpolating the site 552, 502, and 849 records at equal time intervals and calculating $\%UNADW_{502}$ as follows:

$$\%UNADW_{502} = \frac{\delta^{13}C_{502} - \delta^{13}C_{849}}{\delta^{13}C_{552} - \delta^{13}C_{849}} \times 100\%.$$

Values exceeding 100% were assigned a value of 100%. Values of $\%UNADW_{502}$ for the 2 - 1 Ma interval are not calculated, because the results may be seriously compromised due to the bias toward interglacial $\delta^{13}C$ values at site 502 from 2.0 to 1.7 Ma and because the site 552 record contains a gap from approximately 1.62 to 1.32 Ma. The results are plotted against $\delta^{18}O$ for the 2.6-2 Ma interval and the 1-0 Ma interval on Figure 10. It is not clear from Figure 10 whether or not the results from the two intervals differ, so to evaluate whether the $\%UNADW_{502}$ has changed during glaciations or interglaciations, we divide the data for each time interval into two sets, one corresponding to $\delta^{18}O$ data points that are above the midpoint of the $\delta^{18}O$ range for that interval

Table 5. Mean ± 1 Standard Deviation of $\delta^{13}C$ During Interval Indicated

Age, Ma	G	I	G - I
	Site 552		
0 - 1	0.98 ± 0.30(81)	1.03 ± 0.35(72)	-0.05
1 - 2	0.96 ± 0.19(43)	1.03 ± 0.25(61)	-0.07
2 - 2.6	0.71 ± 0.28(28)	0.86 ± 0.23(67)	-0.15
	Site 502		
0 - 1	0.83 ± 0.23(107)	0.74 ± 0.21(56)	0.09
1 - 2*	0.72 ± 0.17(76)	0.70 ± 0.20(121)	0.02
2 - 2.6	0.66 ± 0.14(18)	0.57 ± 0.15(41)	0.09
	Site 607		
0 - 1	0.10 ± 0.49(110)	0.67 ± 0.40(118)	-0.57
1 - 2	0.67 ± 0.39(111)	0.96 ± 0.19(114)	-0.29
2 - 2.6	0.47 ± 0.29(39)	0.87± 0.21(115)	-0.40
	Site 849		
0 - 1	-0.30 ± 0.23(137)	-0.07 ± 0.23(128)	-0.23
1 - 2	-0.29 ± 0.19(151)	-0.03 ± 0.20(126)	-0.26
2 - 2.6	-0.30 ± 0.33(57)	-0.01 ± 0.18(64)	-0.27
	Site 677		
0 - 1	-0.54 ± 0.21(188)	-0.36 ± 0.29(147)	-0.18
1 - 2	-0.60 ± 0.19(169)	-0.43 ± 0.24(184)	-0.17
2 - 2.6	-0.76 ± 0.18(33)	-0.61 ± 0.22(158)	-0.15
	Site 502 - 849		
0 - 1	1.07 ± 0.23	0.77 ± 0.22	0.30
1 - 2*	0.95 ± 0.22	0.72 ± 0.18	0.23
2 - 2.6	0.90 ± 0.22	0.59 ± 0.22	0.31
	Site 552 - 849		
0 - 1	1.21 ± 0.27	1.10 ± 0.21	0.11
1 - 2	1.24 ± 0.23	1.06 ± 0.24	0.18
2 - 2.6	1.07 ± 0.27	0.86 ± 0.22	0.21

Glacial (G) and interglacial (I) points were selected on the basis on their $\delta^{18}O$ values: $\delta^{13}C$ values associated with $\delta^{18}O$ values greater than the midpoint of the $\delta^{18}O$ range for that interval were considered "glacial", and points having lower $\delta^{18}O$ values were considered "interglacial". Number of measurements used for each average is incuded in parentheses. For the 502 - 849 and 552 - 849 differences, both records were interpolated at 5-kyr intervals prior to the analysis, and the $\delta^{18}O$ record of Site 849 was used to separate glacial from interglacial $\delta^{13}C$ values. G - I is the difference between glacial and interglacial points.

*Results from this interval may be biased due to the absence of glacial *C. wuellerstorfi* at 502 from 2.0 - 1.7 m.y. BP.

(glacial points) and one corresponding to $\delta^{18}O$ values that are below that midpoint (interglacial points). The mean and one standard deviation value for the $\%UNADW_{502}$ are given in Table 6 for glacial and interglacial periods for the two time intervals. The calculations suggest that the $\%UNADW_{502}$ has remained approximately constant (~70%) during interglaciations but has risen during glaciations (from about 80 to 90%). Although a Student t-test [*Sokal and Rohlf,* 1969] indicates the glacial means of the two intervals are different at the greater than 95% confidence interval, we suggest that higher resolution records are needed to confirm the increase in glacial %UNADW to the middepth tropical Atlantic. In any case, both glacial and interglacial $\delta^{13}C$ values have increased at site 502 (Figure 9, Table 5), but the $\%UNADW_{502}$ during interglaciations has remained approximately constant (Table 6). Therefore the $\delta^{13}C$ rise at site 502 cannot be attributed entirely to an increase in the $\%UNADW_{502}$.

Finally, we evaluate the remaining possibility, that the $\delta^{13}C$ rise at sites 502 and 552 was due to an increase in the $\delta^{13}C$ value of North Atlantic surface source waters. The $\delta^{13}C$ record of *Neogloboquadrina pachyderma* (sinistral) from Norwegian Sea site 644 (Figure 1), which has a gap between 2.6 and 1.5 Ma,

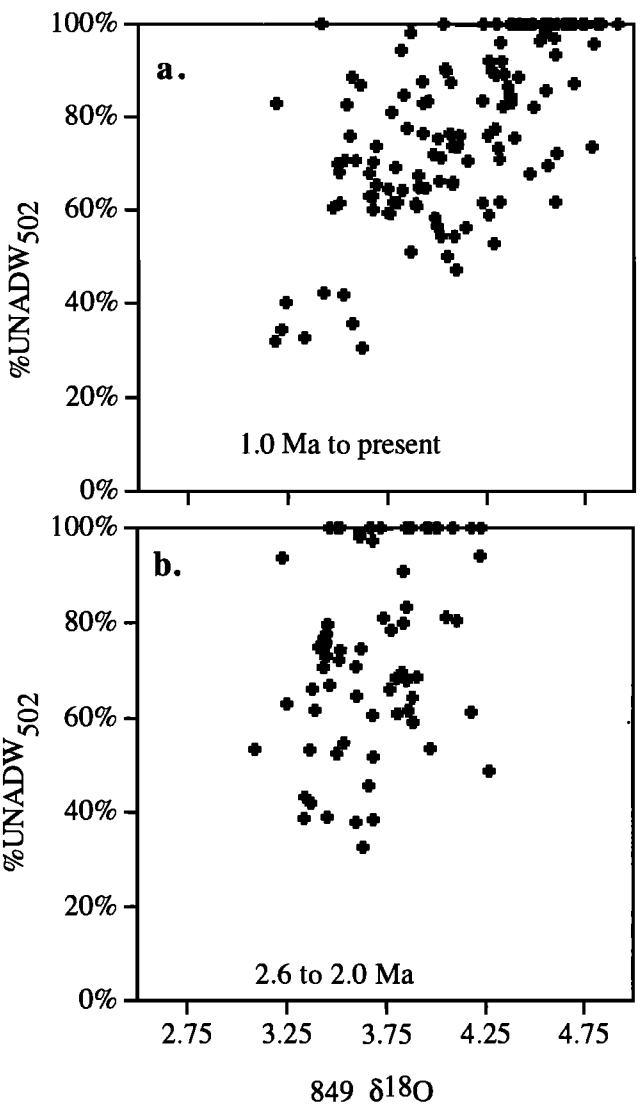

Figure 10. Site 849 $\delta^{18}O$ versus percentage of UNADW for site 502 ($\%UNADW_{502}$) relative to sites 849 and 552, calculated as follows: $\%UNADW_{502} = (\delta^{13}C_{502}-\delta^{13}C_{849})/(\delta^{13}C_{552}-\delta^{13}C_{849}) \times 100\%$. The records were interpolated at 5,000-year intervals prior to subtraction, and sections with data gaps were omitted. Values greater than 100% were set to 100%.

Table 6. Mean and Standard Deviation for Interglacial and Glacial Percentage of UNADW for Site 502 (%$UNADW_{502}$) for the 2.6 - 2 and 1 - 0 Ma Time Intervals

	Mean ± Standard Deviation	
	1 - 0 Ma	2.6 - 2 Ma
Interglacial	67 ± 17	70 ± 21
Glacial	89 ± 24	78 ± 21

Glacial and interglacial points were separated based on $\delta^{18}O$ values: %UNADW values associated with $\delta^{18}O$ values greater than the midpoint of the $\delta^{18}O$ range for that interval were considered "glacial," and points having lower $\delta^{18}O$ values were considered "interglacial." Values greater than 100% were set to 100%.

exhibits a $\delta^{13}C$ increase of up to 1‰ over the past 1.5 m.y. [*Jansen et al.*, 1988]. The $\delta^{13}C$ record of *N. pachyderma* (sinistral), from site 643, also in the Norwegian Sea (Figure 1), exhibits an increase over the past 1 m.y., although it is somewhat smaller than at site 644 [*Jansen, et al.*, 1988]. By contrast, the $\delta^{13}C$ record of *Globigerina bulloides* from subpolar North Atlantic site 610 (Figure 1) shows a 0.5‰ decrease from 2.6 to 0.7 Ma (E. Jansen, unpublished data, 1994). Late Pleistocene $\delta^{13}C$ values of *N. pachyderma* (sinistral and dextral) at site 610 were also lower than latest Pliocene values [*Jansen and Sejrup*, 1987]. One might argue that data from the Norwegian Sea are more relevant, because this is where most deep water forms except perhaps during the coldest glaciations [*Duplessy et al.*, 1992; *Labeyrie et al.*, 1992]. In summary, planktonic $\delta^{13}C$ records from the Norwegian Sea indicate rising $\delta^{13}C$ values over the past 1.5 m.y., consistent with increasing $\delta^{13}C$ values in the source waters for NADW as the explanation for rising $\delta^{13}C$ values at sites 502 and 552. Planktonic $\delta^{13}C$ records spanning the entire past 2.6 m.y. from the Norwegian Sea would be helpful in further assessing this possibility.

Why might northern source water $\delta^{13}C$ values have increased through time? Examination of the evolution of the Atlantic-Pacific $\delta^{13}C$ gradient provides an important constraint when considering this question. Due to the increase in $\delta^{13}C$ values at site 552, the Atlantic-Pacific (552-849) $\delta^{13}C$ gradient was greater in the late Pleistocene than it was in the late Pliocene. *Raymo et al.* [1990] found a smaller gradient in the late Pleistocene, rather than a larger one as we have found here, due to their use of the site 677 record instead of the site 849 record. They used the site 552 records as their northern source end-member as we have here. The increase toward the present in the Atlantic-Pacific $\delta^{13}C$ gradient that we describe here is caused by the increase in $\delta^{13}C$ values at site 552 relative to no increase at site 849, whereas the decrease in the $\delta^{13}C$ gradient described by *Raymo et al.* [1990] is caused by a larger $\delta^{13}C$ increase at site 677 than at site 552 (Figure 9). As discussed above, there are reasons to believe that site 849 $\delta^{13}C$ values are more representative of mean deep Pacific values [*Mix et al.*, 1995].

Assuming that site 849 rather than site 677 represents the mean ocean $\delta^{13}C$ record, several possible reasons exist for the increase in $\delta^{13}C$ values which are consistent with an increase in the Atlantic-Pacific $\delta^{13}C$ gradient. An oceanic nutrient inventory increase, without an associated Redfield ratio carbon increase, may have caused the higher Atlantic $\delta^{13}C$ values and increased $\delta^{13}C$ gradient. For example, assuming that the North Atlantic-Pacific (552-849) $\delta^{13}C$ increase (from 1 ‰ to 1.2 ‰) was proportional to the increase in the $\delta^{13}C$ gradient between nutrient-free surface water and deep Pacific waters, then the latter gradient increased by 20 % or 0.35 ‰, from 1.65 ‰ 2.6 m.y. ago to 2.0 ‰ today. The resulting increase in productivity would have caused $\delta^{13}C$ values to increase in nutrient-poor waters and to decrease in nutrient-rich deep waters. However, a 0.35‰ $\delta^{13}C$ rise in nutrient-poor waters would be associated with only a small $\delta^{13}C$ drop in the greater volume of nutrient-rich waters if mean ocean values remained approximately constant. For example, assuming that the volume ratio of nutrient-poor and nutrient-rich waters was 1:3, then Pacific deepwater $\delta^{13}C$ values would drop by only ~0.1 ‰ to balance a 0.35‰ increase in nutrient-poor waters. Records of surface-dwelling planktonic foraminifera from the western tropical Pacific, however, do not exhibit a $\delta^{13}C$ increase [*Schmidt et al.*, 1990; *Whitman and Berger*, 1990] as would be predicted from this scenario.

If the Atlantic-Pacific (552-849) $\delta^{13}C$ gradient increased due to an increase in whole ocean nutrient and carbon content supplied with the Redfield ratio of organic matter, then, because organic matter has low $\delta^{13}C$ values, the mean ocean $\delta^{13}C$ value should also decrease, unlike the observations at site 849. Mean ocean values would also decrease if there was an increase in the weathering of organic matter relative to that of carbonate. If low-latitude productivity increased in response to greater nutrient concentrations, the nutrient-depleted regions, such as the North Atlantic, should exhibit a smaller $\delta^{13}C$ decrease than the mean ocean (see discussion by *Boyle* [1986]). If the decrease in the mean ocean $\delta^{13}C$ value due to a Redfield ratio nutrient inventory increase was fortuitously balanced by a non-nutrient-related whole ocean $\delta^{13}C$ increase such as might occur due to the growth of the terrestrial biosphere [*Shackleton*, 1977], to a reduction in $\delta^{13}C$ values or C/P ratios of buried organic matter, or to an increase in the weathering of carbonates relative to organic matter, then the Atlantic-Pacific $\delta^{13}C$ gradient could increase without a decrease in Pacific $\delta^{13}C$ values, as is observed. Additional data are needed, both to confirm the increase in source water $\delta^{13}C$ values and to evaluate possible reasons for the increase.

Implications of %$UNADW_{502}$ Changes on Northward Heat Transport

As described above, our $UNADW_{502}$ calculations suggest that the contribution of UNADW to the middepth tropical Atlantic during interglaciations remained approximately constant during the past 2.6 m.y., but the glacial contribution may have risen from about 80% to 90%. By contrast, *Raymo et al.* [1990] found a dramatic reduction (from 80% to 20%) in the glacial contribution of LNADW to the deep North Atlantic (site 607) over the same interval. Northward oceanic heat transport in feed waters for NADW production greatly influence the climate of the high-latitude North Atlantic and surrounding land masses [*Broecker et al.*, 1985], thus it is logical to ask whether these changes in the relative contributions of LNADW and UNADW played a role in the observed increasing glacial severity over the past 2.6 m.y. Unfortunately, to address this question explicitly,

we must know the absolute fluxes of both LNADW and UNADW, and the heat released per unit flux of each component of NADW. While we can assume, for simplicity, that the heat released per unit flux of LNADW and UNADW remained constant through time, we cannot constrain the UNADW and LNADW flux changes that yield the estimated changes in the relative contribution of UNADW and LNADW to sites 502 and 607, respectively.

A recent modeling study by *Rahmstorf* [1994], however, provides insight on northward heat transport under different North Atlantic circulation geometries. Using a coupled ocean-atmosphere model with improved surface heat parameterization replacing the traditional restoring boundary condition on temperature, *Rahmstorf* [1994] produced simulations of deep ocean circulation having three different equilibrium states. Transitions between states were achieved by imposing brief meltwater pulses. One of the three states corresponds to strong LNADW production, with convection reaching the bottom of the North Atlantic. In the other two states, LNADW is not produced, and maximum convection depths reach approximately 3 km. Because of the new surface heat parameterization used in this modeling experiment, surface temperature and heat transport are not specified, but change as a result of deep ocean circulation changes. There were several important finding which bear on our study. The shallower cell corresponded to a cool climate and the deeper convection cell corresponded to a warm climate, in agreement with reconstructions of last glacial versus Holocene circulation [e.g., *Boyle and Keigwin*, 1987; *Duplessy et al.*, 1988; *Oppo and Lehman*, 1993] and with the results of this study. Shallow convection occurred south of deep convection, as has been suggested by the work of *Labeyrie et al.* [1992]. The total flux of NADW was similar for both the warm and cold climate, implying that UNADW circulation was more vigorous during cold climates, as was hypothesized by *Oppo and Lehman* [1993] for the last glaciation. Because the meridional heat transport was found to be a function of the latitude of convection, however, meridional heat transport was significantly lower in the cold climate than in the warm climate simulations. Thus, although we cannot derive measures of changes in the absolute fluxes of UNADW and LNADW through time, the results of *Rahmstorf*'s [1994] modeling study suggest that when UNADW is favored over the production of LNADW, northward heat transport is reduced. Thus it is likely that the changes in relative contributions of LNADW and UNADW to the deep and middepth Atlantic, respectively, over the past 2.6 m.y., described here and by *Raymo et al.* [1990], were coupled to reduced northward heat transport, and played a role in the Northern Hemisphere glacial intensification over this interval. At the very least, gradual shoaling of deep water during glaciations may have provided a positive feedback for cooling which occurred due to other factors.

Summary and Conclusions

Our results from Caribbean site 502 suggest that the tendency for higher glacial than interglacial $\delta^{13}C$ values in the middepth tropical Atlantic has persisted throughout the past 2.6 m.y., largely due to a greater contribution of UNADW during glacial than interglacial intervals. The glacial-interglacial difference in the percentage of NADW to site 502 may have increased slightly over the past 2.6 m.y., due to a small increase, from about 80% to about 90%, in the glacial $\%UNADW_{502}$; the interglacial contribution has remained approximately constant. The small increase in glacial UNADW contribution is in contrast to the much larger decrease in glacial LNADW percentage to the deep North Atlantic, from ~80% during the 2-2.6 Ma interval to ~20% over the past million years [*Raymo et al.*, 1990].

Covariance analysis of $\delta^{18}O$ and $\delta^{13}C$ data from site 552, at 2300 m in the subpolar North Atlantic, indicates that throughout the past 2.6 m.y., there was a tendency for higher glacial than interglacial $\delta^{13}C$ in the middepth Atlantic relative to the deep Pacific. This tendency has weakened toward the present, as low-$\delta^{13}C$ southern source waters have increasingly penetrated northward into the deep north Atlantic and the core of glacial nutrient-depleted, high-$\delta^{13}C$ waters has migrated to shallower depths. From approximately 2.6 to 2.0 Ma, glacial NADW influenced both the deep and middepth North Atlantic. From 2.0 to 1.0 Ma, NADW often shoaled above site 607 (3427 m) but still influenced middepth North Atlantic site 552 [*Raymo et al.*, 1990]. Over the past 1 m.y., and particularly over the past 150 kyr, UNADW occasionally shoaled above 2300 m or formed downstream of site 552 [*Oppo and Fairbanks*, 1990; *de Menocal et al.*, 1992; *Oppo and Lehman*, 1993]. Results of a recent modeling study [*Rahmstorf*, 1994] suggest that this gradual shoaling of NADW during glaciations may have resulted in reduced meridional heat transport and hence may have played a role in the glacial intensification that occurred over the past 2.6 m.y.

Mean $\delta^{13}C$ values have risen by about 0.2 ‰ in both the middepth North Atlantic (site 552) and the middepth tropical Atlantic (Caribbean Sea site 502) over the past 2.6 m.y., apparently not due to a mean ocean $\delta^{13}C$ rise. We have evaluated several explanations for the $\delta^{13}C$ rise. Although a small portion of the rise at site 502 may be due to an increase in northern source water contribution relative to southern sources, it is likely that the relative contribution of northern source waters to site 552 during glaciations has been decreasing. We suggest that a rise in the $\delta^{13}C$ values of the source water must also have occurred. Additional high-resolution paleoceanographic records, especially $\delta^{13}C$ records of planktonic foraminifera from source water regions, are needed to understand the significance of Plio-Pleistocene $\delta^{13}C$ trends.

Acknowledgements. We thank Luping Zou and Susan O'Conner-Lough for microscope work, Rindy Ostermann for overseeing most of the isotope analyses, Bill Curry and Dick Norris for useful discussions and reviews of an earlier version of the manuscript, Nick Shackleton for providing the timescale for site 607, and Eystein Jansen for sharing unpublished data from site 610. Reviews by B. Flower, R. Theideman, and K. Miller are also greatly appreciated. We thank Ernie Joynt for preparing the camera-ready copy. This work was funded by NSF grants OCE90-12279, OCE90-18382, and OCE91-02438. This is WHOI contribution # 8735.

References

Belanger, P. E., W. B. Curry, and R. K. Matthews, Core top evaluation of benthic foraminiferal isotopic ratios for paleoceanographical interpretations, *Palaeogeogr. Palaeoclimat. Palaeoecol., 33*, 205-201, 1981.

Berggren, W. A., Late Pliocene-Pleistocene glaciation, In Laughton, A. S., *et al., Init. Rep. Deep Sea Drill. Proj., 12*, 953-963, 1972.

Berggren, W. A., D. A. Kent, J. J. Flynn, and J. A. van Couvering, Cenozoic geochronology, *Geol. Soc. Am. Bull., 96*, 1407-1418, 1985.

Boyle, E. A., Paired carbon isotope and cadmium data from benthic foraminifera: Implications for changes in oceanic phosphorous, oceanic circulation, and atmospheric carbon dioxide, *Geochim. Cosmochim. Acta, 50*, 265-276, 1986.

Boyle, E. A., Cadmium: Chemical tracer of deepwater paleoceanography, *Paleoceanography, 3*, 471-489, 1988.

Boyle, E. A., and L. D. Keigwin, North Atlantic thermohaline circulation during the past 20,000 years linked to high-latitude surface temperature, *Nature, 330*, 35-40, 1987.

Broecker, W. S., and T. H. Peng, The role of $CaCO_3$ compensation in the glacial to interglacial atmospheric CO_2 change, *Global Biogeochem. Cycles, 1*, 15-29, 1987.

Broecker, W. S., D. M. Peteet, and D. Rind, Does the ocean-atmosphere system have more than one stable mode of operation?, *Nature, 315*, 21-26, 1985.

Broecker, W. S., and T. H. Peng, *Tracers in the Sea*, 690pp., Eldigio Press, New York, 1985.

Curry, W. B., and K. G. Miller, Oxygen and carbon isotopic variation in Pliocene benthic foraminifers of the equatorial Pacific, *Proc. Ocean Drill. Program, Sci. Res., 108*, 157-166, 1989.

Curry, W. B., J. C. Duplessy, L. D. Labeyrie, and N. J. Shackleton, Changes in the distribution of $\delta^{13}C$ of deep water ΣCO_2 between the last glaciation and the Holocene, *Paleoceanography, 3*, 317-342, 1988.

de Menocal, P. B., D. W. Oppo, R. G Fairbanks, and W. L. Prell,, Pleistocene $\delta^{13}C$ variability of North Atlantic intermediate waters, *Paleoceanography, 7*, 229-250, 1992.

Duplessy, J. C., N. J. Shackleton, R. G. Fairbanks, L. Labeyrie, D. W. Oppo, and N. Kallel, Deep water source variations during the last climatic cycle and their impact on the global deep water circulation, *Paleoceanography, 3*, 343-360, 1988.

Duplessy, J. C., L. Labeyrie, A. Juillet-Leclerc, F. Maitre, J. Duprat, and M. Sarnthein, Surface salinity reconstruction of the North Atlantic Ocean during the last glacial maximum, *Oceanol. Acta, 14*, 311-324, 1992.

Hodell, D. A., Late Pleistocene paleoceanography of the South Atlantic sector of the Southern Ocean: Ocean Drilling Project hole 704A, *Paleoceanography, 8*, 47-67, 1993.

Hodell, D. A., and K. Venz, Toward a high-resolution stable isotope record of the Southern Ocean during the Plio-Pleistocene (4.8 - 0.8 Ma), in*The Antarctic Paleoenvironment: A Perspective of Global Change, Part one, Antarct. Res. Ser.*, vol. 56, edited by J. P. Kennett and D. A. Warnke, pp. 265-310, AGU, Washington, D.C., 1992.

Jansen, E., and H. P. Sejrup, Stable isotope stratigraphy and amino-acid empimerization for the last 2.6 m. y. at site 610, holes 610 and 610A, *Initial Rep. Deep Sea Drill. Proj., 94*, 879-887, 1987.

Jansen, E., and J. Sjøholm, Reconstruction of glaciation over the past 6 M.y. from ice-borne deposits in the Norwegian Sea. *Nature, 349*, 600-603, 1991.

Jansen, E., U. Bleil, R. Henrich, L. Krinstad, and B. Slettemark, Paleoenvironmental changes in the Norwegian Sea and the northeast Atlantic during the last 2.8 m.y.: Deep Sea Drilling Project/Ocean Drilling Program sites 610, 642, 643, and 644. *Paleoceanography, 3*, 563-583, 1988.

Keffer, T., D. G. Martinson, and B. H. Corliss, The position of the Gulf Stream during Quaternary glaciations, *Science, 241*, 440-442, 1988.

Keigwin, L. D., Pliocene stable-isotopic record of DSDP Site 606: Sequential events of 18O enrichment beginning at 3.1 Ma, In Ruddiman, W. F., et al., *Init. Rep. Deep Sea Drill. Proj., 94*, 911-920, 1987.

Keigwin, L. D., and E. A. Boyle, Carbon isotopes in deep-sea benthic foraminifera: Precession and changes in low-latitude biomass, in *The Carbon Cycle and Atmospheric CO_2: Natural Variations Archean to Present, Geophys. Monogr. Ser.*, vol. 32, edited by E. T. Sundquist and W. S. Broecker, pp. 319-328, AGU, Washington, D. C., 1985.

Keigwin L. D., and R. C. Thunnell, Middle Pliocene climatic change in the western Mediterranean from faunal and oxygen isotopic trends. *Nature, 282*, 292-296, 1979.

Kent, D. V., and D. Spariosu, Magnetostratigraphy of Caribbean site 502 hydraulic piston cores, *Initial Rep. Deep Sea Drill. Proj., 68*, 419-433, 1982.

Kroopnick, P., The distribution of carbon-13 in the world oceans, *Deep Sea Res., Part A, 32*, 57-84, 1985.

Labeyrie, L. D., J. C. Duplessy, J. Duprat, A. Juillet-Leclerc, J. Moyes, E. Michel, N. Kallel, and N. J. Shackleton, Changes in the vertical structure of the North Atlantic Ocean between glacial and modern times, *Quat. Sci. Rev., 11*, 401-413, 1992.

Loubere, P., Gradual late Pliocene onset of glaciation: A deep-sea record from the Northeast Atlantic, *Palaeogeog. Palaeoclimatol. Palaeoecol., 63*, 327-334, 1988.

Manabe, S., and A. J. Broccoli, The influence of continental ice sheets on the climate of an ice age, *J. Geophys. Res. 90*, 2167-2190, 1985.

Mix, A. C., and R. G. Fairbanks, North Atlantic surface-ocean control of Pleistocene deep-ocean circulation. *Earth Planet. Sci. Lett., 73*, 231-243, 1985.

Mix, A. C., N. G. Pisias, W. Rugh, J. Wilson, A. Morey, and T. K. Hagelberg, Benthic foraminiferal stable isotope record from Site 849, 0-5 Ma: Local and global climate changes, ODP Leg 138, *Sci. Res. Ocean Drill. Program*, in press, 1995

Oppo, D. W., and R. G. Fairbanks, Variability in the deep and intermediate water circulation of the Atlantic Ocean: Northern Hemisphere modulation of the Southern Ocean. *Earth Planet. Sci. Lett. 86*, 1-15, 1987.

Oppo, D. W., and R. G. Fairbanks, Atlantic Ocean thermohaline circulation over the last 150,000 years: Relationship to climate and atmospheric CO_2, *Paleoceanography, 5*, 277-288, 1990.

Oppo, D. W., and S. J. Lehman, Middepth circulation of the subpolar North Atlantic during the Last Glacial Maximum, *Science, 259*, 1148-1152, 1993.

Poore, R. Z., and W. A. Berggren, Late Cenozoic planktonic foraminiferal biostratigraphy and paleoclimatology of Hatton-Rockall Basin: DSDP Site 116, *J. Foraminif. Res., 5*, 270-293, 1975.

Prell, W. B., Covariance patterns of foraminiferal $\delta^{18}O$: An evaluation of Pliocene ice volume changes near 3.2 million years ago, *Nature, 226*, 693-694, 1984.

Rahmstorf, S., Rapid climate transitions in a coupled ocean-atmosphere model, *Nature, 372*, 82-85, 1994.

Raymo, M. E., W. F. Ruddiman, and B. M. Clement, Pliocene-Pleistocene paleoceanography of the North Atlantic at Deep Sea Drilling Project Site 609. *Init.ial Rep. Deep Sea Drill. Proj., 94*, 895-901, 1986.

Raymo, M. E., W. F. Ruddiman, J. Backman, B. M. Clement, and D. G. Martinson, Late Pliocene variation in northern hemisphere ice sheets and North Atlantic Deep Water circulation, *Paleoceanography, 4*, 413-446, 1989.

Raymo, M. E., W.F. Ruddiman, N. J. Shackleton, and D. W. Oppo, The evolution of Atlantic-Pacific $\delta^{13}C$ gradients over the last 2.5 M.y.: Evidence for decoupling of deep ocean circulation and global ice volume changes, *Earth Planet. Sci. Lett., 97*, 353-368, 1990.

Raymo, M. E., D. Hodell, and E. Jansen, Response of deep ocean circulation to initiation of northern hemisphere glaciation (3-2 Ma), *Paleoceanography, 7*, 645-672, 1992.

Ruddiman, W. F., A. McIntyre, and M. Raymo, Matuyama 41,000-year cycles: North Atlantic Ocean and northern hemisphere ice sheets, *Earth Planet. Sci. Lett. 80*, 117-129, 1986.

Ruddiman, W. F., M. E. Raymo, D. G. Martinson, B. M. Clement, and J. Backman, Pleistocene evolution of northern hemisphere climate, *Paleoceanography, 4*, 353-412, 1989.

Schmidt, H., W. H. Berger, T. Bickert, and G. Wefer, Quaternary carbon isotope record of pelagic foraminifers: Site 806, Ontong Java Plateau, *Proc. Ocean Drill. Program, Sci. Res. 130*, 381-396, 1990.

Shackleton, N. J., Carbon-13 in *Uvigerina*: Tropical rainforest history and

the equatorial Pacific carbonate dissolution cycles, in *The Fate of Fossil Fuel CO_2 in the Oceans*, edited by N. R. Anderson and A. Malahoff, pp. 401-428, Plenum, New York, 1977.

Shackleton, N. J., and M. A. Hall, Oxygen and carbon isotope stratigraphy of Deep Sea Drilling Project Hole 552A: Plio-Pleistocene glacial history, *Initial Rep. Deep Sea Drill. Proj., 81*, 599-610, 1984.

Shackleton, N. J., and N. D. Opdyke, Oxygen isotope and paleomagnetic stratigraphy of equatorial Pacific core V28-238: Late Pliocene to latest Pleistocene, in Investigations of Late Quaternary Paleoceanography and Paleoclimatology, edited by R. M. Cline and J. D. Hays, *Mem. Geol. Soc. Am., 145*, 449-464, 1979

Shackleton, N. J., A. Berger, and W. R. Peltier, An alternative astronomical calibration of the lower Pleistocene timescale based on ODP Site 677, *Trans. R. S. Edinburgh Earth Sci., 81*, 251-261, 1990.

Shackleton, N.J, and the Leg 81 Shipboard Scientific Party,Oxygen isotope calibration of the onset of ice-rafting and history of glaciation in the North Atlantic region, *Nature, 307*, 620-623, 1984.

Sokal, R. R., and F. J. Rohlf, *Biometry*, 765pp., W.H Freeman, New York, 1969.

Thunnell, R. C., and D. F Williams, The stepwise development of Pliocene-Pleistocene paleoclimatic and paleoceanographic conditions in the Mediterranean: Oxygen isotopic studies of DSDP Sites 125 and 132, *Utrecht Micropaleontol Bull., 30*, 111-118, 1983.

Whitman, J M , and W. H. Berger, Pliocene-Pleistocene carbon isotope record, Site 586, Ontong Java Plateau, *Proc. Ocean Drill. Program, Sci. Res., 130*, 333-348, 1990.

Wüst, G., *Stratification and Circulation of the Antillean-Caribbean Basins, Part 1; Spreading and Mixing of the Water Types with an Oceanographic Atlas*, 202 pp., Columbia University Press, New York, 1964.

G. P. Lohmann and D. W. Oppo, Woods Hole Oceanographic Insttution, Clark Building, Woods Hole, MA 02543. (e-mail: pat@ale.whoi.edu, doppo@whoi.edu)

A. C. Mix, College of Oceanography, Oregon State University, Oceanography Administration Building 104, Corvallis, OR 97331-5503. (e-mail: mix@oce.orst.edu)

W. L. Prell, Department of Geological Science, Brown University, POB 1846, Providence, RI 02912-1846.

M. E. Raymo, Department of Earth, Atmospheric, and Planetary Science, Massachustetts Institute of Technology, Cambridge, MA 02139 (e-mail: raymo@mit.edu)

J. D. Wright, Sawyer Environmental Research Center, University of Maine, Orono, ME 04469 (e-mail: jwright@maine.maine.edu)

(Received June 8, 1994; revised January 18, 1995;
accepted January 19, 1995.)